Cell Communication and Signaling

RESEARCH

Open Access

Induction of LY6E regulates interleukin-1β production, potentially contributing to the immunopathogenesis of systemic lupus erythematosus

Jenn-Haung Lai[1*], De-Wei Wu[1], Chuan-Yueh Huang[2], Li-Feng Hung[2], Chien-Hsiang Wu[1], Shuk-Man Ka[3], Ann Chen[4], Jing-Long Huang[5,6] and Ling-Jun Ho[2*]

Abstract

Systemic lupus erythematosus (SLE) is an autoimmune disorder characterized by the deposition of immune complexes (ICs) in various organs, especially the kidney, leading to lupus nephritis, one of the major and therapeutically challenging manifestations of SLE. Among the various cytokines induced in SLE, type I interferons (IFN-Is) play crucial roles in mediating immunopathogenesis, and anti-IFN-I treatment has been approved for SLE treatment. The uptake of ICs by macrophages results in macrophage activation, which initiates, triggers, and exaggerates immune responses in SLE. After observing the induction of an IFN-stimulated gene, LY6E, in monocytes from SLE patients, we demonstrated the colocalization of both LY6E and a macrophage marker in kidneys from pristane-induced lupus-prone mice and from patients with lupus nephritis. By studying mouse bone marrow-derived macrophages, we showed that LY6E regulated IFN-α- and IC-induced production and secretion of mature interleukin-1β (mIL-1β), foam cell formation and several mitochondria-associated mechanisms, such as the release of mitochondrial DNA (mtDNA) but not mitochondrial RNA (mtRNA) into the cytosol, the generation of mitochondrial reactive oxygen species (mtROS) and ROS, the activation of caspase 1, NLRP3, and the stimulator of interferon genes (STING) signaling pathway, and the activation of cytidine/uridine monophosphate kinase 2 (CMPK2), which were involved in LY6E-mediated immunomodulatory effects. In addition, synergistic effects of a combination of IL-1β and IFN-α and of IL-1β and ICs on the induction of the expression of IFN-stimulated genes were observed. In addition to revealing the proinflammatory roles and mechanisms of LY6E in macrophages, given that various subgroups of macrophages have been identified in the kidneys of patients with lupus nephritis, targeted treatment aimed at LY6E may be a potential therapeutic for lupus nephritis.

Keywords Systemic lupus erythematosus, Macrophages, LY6E, Lupus nephritis, Interferon-alpha, Interleukin-1

*Correspondence:
Jenn-Haung Lai
laiandho@gmail.com
Ling-Jun Ho
lingjunho@nhri.org.tw
Full list of author information is available at the end of the article

Introduction

Systemic lupus erythematosus (SLE) is an autoimmune disease with various clinical presentations involving different organ systems, such as the skin, joints, hematopoietic system, cardiopulmonary system, neurologic system, and kidneys. The etiology of SLE remains unclear, and both genetic and environmental factors are recognized as being responsible for the development of the disease [1]. One of the major clinical manifestations of SLE is lupus nephritis, a disorder characterized by the deposition of immune complexes (ICs) and complement in the kidneys, leading to kidney damage [2]. While cytokines play major roles in most autoimmune diseases, type I interferons (IFN-Is) are likely the most critical cytokines mediating the immunopathogenesis of SLE [3–6]. Increased IFN-I signatures are also commonly detected in the kidney tissues of lupus-prone mice and SLE patients [6]. The success of anti-IFN-I treatment in patients with SLE led to the approval of the anti-IFN-I biologic anifrolumab by the FDA to treat patients with moderate to severe disease [7–9].

An increasing number of studies indicate that, in addition to regulating metabolism, mitochondria can provide a source of disease-associated molecular patterns (DAMPs) and initiate inflammatory reactions [10–12]. Indeed, mitochondria are important organelles that participate in the immunopathogenesis of SLE through, for example, the release of immunogenic mediators such as mitochondrial DNA (mtDNA). mtDNA from engulfed red blood cells by monocytes/macrophages or from neutrophil extracellular traps also serves as a potent inducer of IFN signaling through activating toll-like receptor (TLR)−9 and the cyclic GMP-AMP synthase (cGAS)-stimulator of interferon genes (STING) signaling pathway [13, 14]. In addition, mtDNA can stimulate strong proinflammatory effects through interactions with pattern recognition receptors (PRRs), such as the NLRP3 inflammasome, leading to interleukin-1 (IL-1) production [15].

An examination of both MRL/lpr and pristane-induced lupus-prone mice revealed a positive correlation between the IL-1β level and disease severity and progression, and IL-1β deletion significantly attenuated the serum levels of anti-double-stranded DNA (anti-dsDNA) antibodies (Abs) and proinflammatory cytokines [16–18]. In addition, serum concentrations of IL-1β are significantly greater in Caucasian SLE patients than in controls [19]. Furthermore, IL-1β levels are higher in patients positive for dsDNA Abs than in those that are negative for dsDNA Abs, and there is a higher ratio of IL-1β/IL-12p70 in patients with renal involvement than in those without renal involvement [19]. Moreover, the induction and activation of IL-1 family cytokines could be readily detectable in patients with SLE, which is also correlated with disease severity and organ involvement [20]. Notably, monocytes can coproduce IFN and IL-1β upon opsonization of mitochondria-retaining red blood cells [21]. Earlier studies by Kahlengerg et al. demonstrated that caspase 1 deficiency helps to protect against vascular dysfunction and abrogates the development of IC-deposition glomerulonephritis in pristane-induced mice [22]. Consistent with these results, the inhibition of the NLRP3/ASC/caspase 1 pathway was revealed to significantly reduce the severity of nephritis and anti-dsDNA antibody production in MLR/lpr mice [23]. These studies highlight the important role of IL-1 in the immunopathogenesis of lupus nephritis. Although not assessed on large scales, the effectiveness of anti-IL-1 treatment with anakinra has been observed on various disorders of SLE patients, especially those presenting with macrophage activation syndrome [24–27]. Indeed, anti-IL-1 treatment has been recognized as the first-line treatment for patients with systemic juvenile idiopathic arthritis-associated macrophage activation syndrome [28].

The lymphocyte antigen 6 family member E (LY6E) belongs to the superfamily of LY6 urokinase-type plasminogen activator receptor proteins and encodes a glycosylphosphatidyl-inositol (GPI)-anchored cell surface protein [29]. *LY6E* gene expression can be detected in macrophages and various immune cells and appears to play a role in the proliferation and differentiation of immune cells [30, 31]. Although many studies have explored the roles of LY6E in virus infection and cancer [29, 32, 33], the significance of this molecule in autoimmune diseases such as SLE remains largely unknown. Our preliminary observations revealed the induction of *LY6E* mRNA, among several highly induced genes, in the monocytes of SLE patients compared with those of healthy controls [34]. This finding supports those of an earlier study showing increased expression of *LY6E* mRNA, among five studied IFN-I-inducible genes, in the whole blood cells of SLE patients, and *LY6E* mRNA levels correlated with the severity of proteinuria, revealing the usefulness of LY6E in distinguishing active lupus nephritis from inactive lupus nephritis [35]. In the present study, in addition to showing an increase in LY6E-positive macrophages in kidney tissues from pristane-induced lupus model mice and from patients with lupus nephritis, we explored the mechanisms responsible for LY6E-regulated proinflammatory responses and IL-1β production in primary mouse bone marrow-derived macrophages (BMDMs).

Materials and methods

Reagents

All the information about the Abs used in this study is detailed in Supplementary Table 1. MitoSOX (M36008), JC-1 (M34152), and H2DCFDA (D399) were purchased from Thermo Fisher Scientific (Waltham, MA, USA). Recombinant mouse IFN-α (12,100–1) was purchased from PBL Assay Science (Piscataway, NJ, USA). Recombinant mouse interleukin (IL)−1β (400-ML-010) and recombinant mouse macrophage migration inhibitory factor (MIF) (1978-MF-025) were purchased from R&D, Inc. (New York, NY, USA). Recombinant mouse IFN-γ (315–05), recombinant mouse IFN-λ2 (250–33), recombinant mouse IL-4 (214–14), recombinant mouse IL-10 (210–10), recombinant mouse IL-6 (216–16) and recombinant mouse tumor necrosis factor (TNF)-α (315-01A) were purchased from PeproTech, Inc. (Rehovot, Israel). Oxidized low-density lipoprotein (OxLDL) (770,252) was purchased from KALEN Biomedical (Montgomery Village, MD, USA). Lipopolysaccharide (LPS) (tlrl-3pelp), Pam3CSK4 (tlrl-pms), PolyIC (tlrl-picw), R848 (tlrl-r848), CpG ODN1826 (tlrl-1826), H151 (inh-h151), Ac-YVAD-cmk (HY-16990) and voltage-dependent anion channel oligomerization inhibitor (VBIT-4, HY129122) were purchased from MedChemExpress LLC (Monmouth Junction, NJ, USA). The FAM-FLICA® Caspase-1 Assay Kit was purchased from Immunochemistry Technologies (Davis, CA, USA). A mitophagy detection kit (MD01), MT-1 MitoMP Detection Kit (MT13) and LDH release assay kit (CK12) were purchased from Dojindo (Kumamoto, Japan). MitoTracker Green FM (M7514) was purchased from Thermo Fisher Scientific. Human CD14 + microbeads (130–050–201) and FcR Blocking Reagent (130–092–575) were purchased from Miltenyi Biotec (Bergisch Gladbach, North Rhine-Westphalia, Germany). Unless otherwise specified, all other reagents were purchased from Sigma–Aldrich.

Preparation of human primary cells and mouse bone marrow-derived macrophages (BMDMs)

Peripheral blood mononuclear cells (PBMCs) were prepared from the buffy coat, and $CD14^+$ monocytes were positively selected from among the PBMC populations of SLE patients or healthy controls with a MACS cell isolation column (Miltenyi Biotech, Auburn, USA) as described in our previous report [36]. A diagnosis of SLE was based on 1982 diagnostic criteria, and the use of human blood samples was approved by the IRB (no. 201509825A3) of Chang Gung Memorial Hospital, Linko, Taiwan. For the preparation of mouse BMDMs, male C57BL/6 mice (6–12 wks) were purchased from the National Laboratory Animal Breeding and Research Center (Taipei, Taiwan). All the animal studies were conducted in accordance with a protocol approved by the Institutional Animal Care and Use Committee of the NHRI (NHRI-IACUC-111045-AC1-M1-A). The bone marrow was flushed from the tibias and femurs of the hind legs of the mice with DMEM with a needle syringe. After being washed and filtered through a 40-μm nylon cell strainer, the mouse bone marrow cells were cultured in DMEM containing 10% FBS and 15% L929 cell-conditioned media for 7 days, and the culture medium was changed every 2–3 days to obtain BMDMs [37].

Pristane-induced lupus mice

Pristane-induced lupus-prone mice were generated according to the method described by Satoh and Reeves [38]. Female BALB/c mice (6 wks old) were purchased from BioLASCO Taiwan Co., Ltd. Mice were randomly separated into groups for pristane (0.5 ml/mouse, CDX-P0161, AdipoGen) or phosphate-buffered saline (PBS) intraperitoneal (i.p.) injection. The mice were sacrificed at 7 months after treatment. All the animal studies were conducted in accordance with a protocol approved by the Institutional Animal Care and Use Committee of the NHRI (NHRI-IACUC-111045-AC1-M1-A).

Serum antibody detection with enzyme-linked immunosorbent assays

Serum levels of antinuclear Abs (ANAs) in mice were measured with enzyme-linked immunosorbent assay (ELISA) kits purchased from Alpha Diagnostic International (catalog no. 5210) according to the manufacturer's instructions.

Histology

Kidney tissues were fixed overnight with a 10X volume of 10% (w/v) neutral buffered formalin at 4 °C. The 0.5 cm thick tissue samples were then stored in 75% ethanol, embedded in paraffin and stained with hematoxylin and eosin. The sections were observed under a light microscope (Leica DM2500 Upright Fluorescence Microscope). Pictures were taken by using an Olympus cooled digital color camera DP73 and analyzed with cellSens life science imaging software. Human paraffin-embedded tissue sections were purchased from BioChain Institute, Inc. (kidney sample from a 36-year-old lupus nephritis patient, Cat. T2236142Lup, Lot. C409066) and TissueArray.Com LLC (normal kidney tissue array, KDN242).

Immunohistochemical staining and confocal microscopic analysis

The sections were deparaffinized with xylene and rehydrated in graded alcohols and distilled water according to previous methods [39]. For antigen retrieval, the slides

were placed in antigen unmasking solution (Vector-Lab, H-3300, citrate-based, pH 6.0) or antigen retrieval buffer (Abcam, AB93684, Tris–EDTA buffer, pH 9.0) for 10 min in a pressure cooker, and then, the samples were cooled for 30 min. After being blocked with PBS containing 3% BSA and 10% normal goat or donkey serum for 30 min, the slides were incubated with primary Abs, including anti-LY6E, anti-CD68 (for human samples) and anti-F4/80 (for mouse samples) Abs, overnight at 4 °C in a wet chamber in the dark. After washing, secondary Abs conjugated with fluorescent dye were added, and the samples were incubated for 1 h in the dark at room temperature with occasional mixing. The cell nuclei were counterstained with Nuclear Violet DCS1. Finally, the sections were mounted with mounting reagent (ProLong Diamond Antifade Mountant, Thermo Fisher Scientific) for analysis with a Leica TCS SP5II and Stellaris 8 confocal laser-scanning microscope (Leica Microsystems, Wetzlar, Germany) equipped with HC PL APO 20×/0.75 IMM CORR CS2 and HC PL APO 63×/1.30 GLYC CORR CS2 objectives (Leica) in the core facilities of the NHRI according to our previous report [36]. 3D reconstructed z-stack images and colocalization analysis were performed with Imaris imaging software (Oxford Instruments) and LAS X Life Science microscope software.

Preparation of cytosolic and mitochondrial fractions

A Mitochondria/Cytosol Fractionation Kit from Abcam (Cambridge, UK) was used to extract the mitochondrial and cytosolic fractions [34]. In brief, 7–10×10^6 cells were resuspended in 0.5 ml of 1X Cytosol Extraction Buffer Mix supplemented with dithiothreitol (DTT) and protease inhibitors. After incubation on ice for 10 min, the cells were homogenized in an ice-cold Dounce tissue homogenizer (150–200 passes with a grinder). The homogenate was centrifuged at 700×g in a microcentrifuge for 10 min at 4 °C, and the supernatant was then centrifuged at 10,000×g in a microcentrifuge for 30 min at 4 °C. The supernatant was then collected (cytosolic fraction), and the pellet (intact mitochondria) was resuspended in 50–70 µl of the Mitochondrial Extraction Buffer Mix supplemented with DTT and protease inhibitors (mitochondrial fraction).

siRNA transfection

The cells were collected and resuspended at 1×10^7/ml in modified Eagle's minimum essential medium (Opti-MEM, Invitrogen) supplemented with 300 nM siRNA as indicated (Stealth RNAi™ siRNA, Invitrogen) [37]. Electroporation was performed with a BTX electroporator (San Diego, CA) with one pulse of 300 V administered for 3 ms [36]. The cells (2×10^6) were then cultured in DMEM (Invitrogen, Carlsbad, CA, USA) supplemented with 10% FBS for 24 h for subsequent experiments. The sequence of the *Ly6e* siRNA was GUACCAAACUCA CCCAUAC, and that of the *CMPK2* siRNA was GGC AGUACUUGACCUAGUU.

Overexpression of CMPK2

The mouse *Cmpk2-DYK* and *DYK* genes were purchased from GenScript. Inc. (Piscataway, NJ) and subcloned and inserted into the PLKO_AS3w.puro. lentivector according to previously outlined methods [40]. The correctness of the subcloning was confirmed by sequencing. To overexpress CMPK2 in cells, BMDMs were transduced with the lentivirus (MOI of 2), and 8 µg/ml polybrene was added. After 48 h, the medium was replaced with fresh medium, and the cells were then used for the designated experiments.

Intracellular reactive oxygen species measurements

After treatment, 2×10^6 adherent BMDMs were washed with PBS prior to incubation with 10 µM H_2DCFDA for 30 min at 37 °C. The cells were then detached and centrifuged at 1000 rpm for 5 min, resuspended in PBS, and analyzed with a flow cytometer (Becton Dickinson) for the measurement of intracellular reactive oxygen species (ROS) levels.

Extraction of total DNA, cytosolic DNA and cytosolic DNA

The BMDMs (4×10^6) were divided into two equal aliquots. One aliquot, which was used as the normalization control, was used to extract total DNA with a NucleoSpin Tissue Kit (Macherey–Nagel, Duren, Germany). The other aliquot was resuspended in 400 µl of buffer comprised of 150 mM NaCl, 50 mM HEPES, pH 7.4, and 25 µg/ml digitonin (EMD Chemicals, Gibbstown, NJ, USA). The samples were rotated end-over-end for 15–20 min at 4 °C and then centrifuged at 980×g three times for 3 min each time to remove cellular debris. The supernatants were collected and poured into fresh tubes and then spun at 17,000×g for 10 min to remove any remaining cellular residue and obtain a cytosolic fraction not contaminated with nuclei, mitochondria, or endoplasmic reticula. The DNA in the cytosolic fraction was then isolated by running the sample through a NucleoSpin Tissue column (Macherey–Nagel) and subsequently eluted with buffer. For fractionating cytoplasmic mtRNA**,** BMDMs (2×10^6) were resuspended in 400 µl of buffer containing 150 mM NaCl, 50 mM HEPES (pH 7.4), and 25 µg/ml digitonin (EMD Chemicals, Gibbstown, NJ, USA). After end–over-end rotation for 15–20 min at 4 °C, the samples were centrifuged at 980×g three times for 3 min each time to remove cellular debris. The supernatants were collected, poured into fresh tubes and then spun at 17,000×g for 10 min to remove remaining

cellular residues. After this, a cytosolic fraction without contaminating the cellular nuclei, mitochondria, or endoplasmic reticulum was obtained. The fractions were subjected to RNA purification by RNAspin Mini (Cytiva), and equal volumes of eluate were used for cDNA production and subsequent analysis by RT–qPCR.

Quantitative RT–qPCR and mtDNA and mtRNA measurements

Total RNA from treated cells was isolated with NucleoZol reagent (Macherey–Nagel, Duren, Germany). The RNA concentrations were measured with a NanoDrop spectrophotometer (ND 1000 V.3.1.0; Thermo Fisher Scientific, Waltham, MA, USA). Reverse transcription was performed in a 20-µl mixture supplemented with 2 µg of total RNA, random hexamers (Invitrogen), a mixture comprised of 10× reverse transcription buffer, dNTPs, magnesium chloride, and dithiothreitol (Invitrogen), and Moloney murine leukemia virus reverse transcriptase (MMLV RTase; Invitrogen). cDNA was prepared for further measurements by qPCR. Briefly, 20 ng of cDNA was amplified in a total mixture volume of 20 µl consisting of 1× KAPA SYBR FAST qPCR Master Mix (KAPA Biosystems, Boston, MA, USA) and the appropriate gene-specific primers, which were added to a final concentration of 200 nM. The primers used are shown in Table 1. The reactions were performed in 40 cycles of 95 °C for denaturation and 60 °C for annealing and extension on a LightCycler 480 (Roche). The changes in gene expression were calculated with the following formula: fold change = $2^{-(\Delta Ct)}$, where ΔCt = Ct of the target gene − Ct of the housekeeping gene. The fold changes were divided by the mean of control replicates. To measure the levels of mtDNA, 20 ng of isolated DNA was subjected to qPCR with KAPA SYBR FAST qPCR Master Mix (KAPA Biosystems) and 200 nM mtDNA primers or nuclear DNA (nDNA) primers. Two mtDNA primer pairs were used to quantify the mtDNA. The levels of mtDNA in the total cell lysate were calculated as the level of mtDNA normalized to the level of nDNA. To quantify the mtDNA in the cytosolic fraction, 20 ng of a purified plasmid (pCR3.1-flag) was added to the eluted solution as described in our previous report [36]. Specific primers for both endogenous mtDNA and the pCR3.1-flag plasmid were used to measure the relative content of cytosolic mtDNA normalized to that of pCR3.1-flag. The relative mtDNA abundance indicates the relative mtDNA content in treated cells normalized to that in nontreated cells. To determine cytosolic mtRNA, qPCR was performed with primers specific for mitochondrial *Nd1* and *Cox2* cDNA, which had been reverse-transcribed from RNA isolated from the cytosolic fraction. In these cases, values were normalized to those of a housekeeping control gene (HPRT).

Western blotting

Enhanced chemiluminescence Western blotting (Amersham, GE Healthcare Life Sciences, Uppsala, Sweden) was performed as previously described [41]. Briefly, cellular proteins or concentrated supernatants were prepared, separated on SDS–PAGE gels and transferred to a nitrocellulose membrane. For immunoblotting, the nitrocellulose membrane was incubated with TBS-T supplemented with 5% nonfat milk for 1 h and then blotted with Abs against individual proteins for 2 h at room temperature or overnight at 4 °C. After washing with TBS-T, the membrane was incubated with secondary Abs conjugated to horseradish peroxidase for 1 h. The membrane was then incubated with the substrate and exposed to X-ray film. After scanning, the intensities of the bands were measured with ImageJ software.

Flow cytometry

The methods for determining the expression of cell surface markers have been previously described [36]. The cells were collected, washed twice with cold PBS and then stained with immunofluorescence dye-conjugated Abs in the presence of blocking reagent to identify cell surface markers at 4 °C for 30 min. The cells were then analyzed, and the signals of the targeted molecules were quantified by flow cytometry (FACSCalibur or BD Accuri™ C6, BD Biosciences).

Oil Red O staining

Oil Red O staining was performed according to methods in our previous report [37]. After treatment, the cells were washed with PBS and then fixed with 10% formalin. After the formalin was removed, the cells were pretreated with 60% isopropyl alcohol and stained with 0.2% Oil Red O solution (Sigma–Aldrich) in 60% isopropyl alcohol. The cells were examined by light microscopy (400X), and the percentages of Oil Red O-positive cells in 5 microscopic fields for each independent experiment were determined and calculated.

BODIPY dye staining

For intracellular staining of neutral lipid proteins, the collected cells were washed twice with cold PBS before being fixed with 4% paraformaldehyde [37]. After 24 h of incubation at 4 °C, the cells were stained with 0.5 µM fluorescent neutral lipid dye 4,4-difluoro-1,3,5,7,8-pentamethyl-4-bora-3a,4a-diaza-s-indacene (BODIPY 493/503) (Molecular Probes, Eugene, OR, USA) and incubated for 20 min at 37 °C. After the cells were washed with PBS and detached with 0.5 mM EDTA (Invitrogen), the level of neutral lipids in the cells was quantified by flow cytometry.

Table 1 Summary of primer sequences used in the study

Gene name	Accession number	Primer-forward	Primer-reverse
(Homo sapiens)			
LY6E	NM_002346.3	AGGCTGCTTTGGTTTGTGAC	AGCAGGAGAAGCACATCAGC
CMPK2	NM_207315.4	AGGTGAAGGTCGGAGTCAAC	CCATGTAGTTGAGGTCAATG AAGG
USP18	NM_017414.3	CCTGAGGCAAATCTGTCAGTC	CGAACACCTGAATCAAGGAGTTA
GAPDH	NM_001289746.1	AGGTGAAGGTCGGAGTCAAC	CCATGTAGTTGAGGTCAATGAAGG
IFN-α	NM_024013.3	TGGAAGCCTGTGTGAT	ATGATTTCTGCTCTGACA
IFN-γ	NM_000619.3	AGCTCTGCATCGTTTTGGGTT	GTTCCATTATCCGCTACATCTGAA
IFN-λ	NM_172140.2	GAGGCCCCCAAAAAGGAGTC	AGGTTCCCATCGGCCACATA
(Mus musculus)			
LY6E	NM_008529.4	ATCTTCGGGGCCTCTTCAC	ATGAGAAGCACATCAGGGAAT
LY6D	NM_010742	CATGCTTTAGCCATGATGGAGGC	ATGTCATCAGCTCTTGGTGCCC
CMPK2	NM_020557.4	GGAACCTCATCTGCACCCAT	GTGGTCTTACCAGTGGCATCC
IFN-α	NM_010503.2	AAGGACAGGCAGGACTTTGGATTC	GATCTCGCAGCACAGGGATGG
IFN-β1	NM_010510.2	CAGCTCCAAGAAAGGACGAAC	GGCAGTGTAACTCTTCTGCAT
USP18	NM_011909	GGAACCTGACTAAGGACCAGATC	GAGAGTGTGAGCAGTTTGCTCC
IL-18	NM_008360	GACAGCCTGTGTTCGAGGATATG	TGTTCTTACAGGAGAGGGTAGAC
CCL5	NM_013653	CCTGCTGCTTTGCCTACCTCTC	ACACACTTGGCGGTTCCTTCGA
IL-8 (CXCL15)	NM_011339	GGTGATATTCGAGACCATTTACTG	GCCAACAGTAGCCTTCACCCAT
RIG1(DDX58)	NM_172689	AGCCAAGGATGTCTCCGAGGAA	ACACTGAGCACGCTTTGTGGAC
MDA5(IFIH1)	NM_027835	TGCGGAAGTTGGAGTCAAAGCG	CACCGTCGTAGCGATAAGCAGA
ISG15	NM_015783	CAATGGCCTGGGACCTAAA	CTTCTTCAGTTCTGACACCGTCAT
RSAD2	NM_021384	AACAGGCTGGTTTGGAGAAGATC	TCCTCCTTGCAGAATCTCACAA
IFITM3	NM_025378	TTCTGCTGCCTGGGCTTCATAG	ACCAAGGTGCTGATGTTCAGGC
CXCL10	NM_021274	ATCATCCCTGCGAGCCTATCCT	GACCTTTTTTGGCTAAACGCTTTC
MX1	NM_010846.1	GGGGAGGAAATAGAGAAAATGAT	GTTTACAAAGGGCTTGCTTGCT
IFIT1	NM_008331.4	CAAGGCAGGTTTCTGAGGAG	GACCTGGTCACCATCAGCAT
TNF-α	NM_013693	CTGAACTTCGGGGTGATCGG	GGGAGTAGACAAGGTACAACCC
IL-6	NM_031168	GACTTCACAGAGGATACCAC	GTACTCCAGAAGACCAGAGG
IL-1β	NM_008361	TTGACGGACCCCAAAAGATGAAGGG	TCCACAGCCACAATGAGTGATACTG
TFAM	NM_009360	GAGGCAAAGGATGATTCGGCTC	CGAATCCTATCATCTTTAGCAAGC
PGC1α	NM_008904	GAATCAAGCCACTACAGACACCG	CATCCCTCTTGAGCCTTTCGTG
NRF1	NM_010938	GGCAACAGTAGCCACATTGGCT	GTCTGGATGGTCATTTCACCGC
NRF2	NM_010902	CCAGCTACTCCCAGGTTGC	CCAAACTTGCTCCATGTCCT
PPARγ	NM_011146	GTACTGTCGGTTTCAGAAGTGCC	ATCTCCGCCAACAGCTTCTCCT
SOD1	NM_011434	GGTGAACCAGTTGTGTTGTCAGG	ATGAGGTCCTGCACTGGTACAG
SOD2	NM_013671	TAACGCGCAGATCATGCAGCTG	AGGCTGAAGAGCGACCTGAGTT
DRP1	NM_152816	GCGAACCTTAGAATCTGTGGACC	CAGGCACAAATAAAGCAGGACGG
MFN1	NM_024200	CCAGGTACAGATGTCACCACAG	TTGGAGAGCCGCTCATTCACCT
HPRT	NM_013556	GCTGGTGAAAAGGACCTCT	CACAGGACTAGAACACCTGC
OGG1	NM_010957	TGAGCTGCGTCTGGACTTGGTT	CTCCGTCTGAGTCAGTGTCCAT
C5aR1	NM_007577	CCATTAGTGCCGACCGTTTCCT	CACGAAGGATGGAATGGTGAGG
C5aR2	NM_176912	GGAGACCTCTTCCTACTGGCTT	AGCCTACGGTAGACAGCAGAAG
mt-ND1	KY018919.1	CTAGCAGAAACAAACCGGGC	CCGGCTGCGTATTCTACGTT
Actin	NC_000071.6	AAAGCCGTATTAGGTCCATCTTGA	GGCCATTGAGGCGTGATC
mt-COX2	KY018919.1	CCTGGTGAACTACGACTGCT	GGACTGCTCATGAGTGGAGG
pCR3.1-Flag		GAAAAGTGCCACCTGACGC	GCCCCCGATTTAGAGCTTGA

Mitochondrial ROS measurements

For mitochondrial ROS (mtROS) measurement, the cells were incubated with 5 μM MitoSOX™ Red (Invitrogen) in culture medium for 30 min at 37 °C. After being washed with PBS, the cells were analyzed by flow cytometry [36].

Mitochondrial membrane potential measurement

The mitochondrial membrane potential was determined with an MT-1 MitoMP Detection Kit (MT13; Dojindo) and MitoTracker Green FM (MTG) (M7514; Invitrogen) according to the manufacturers' instructions. In brief, BMDMs (2×10^6 cells per condition) were incubated with MT-1 solution (1:1000) and MTG (100 nM) for 30 min at 37 °C. After the cells were washed with PBS, the fluorescence intensity of MT-1 and MTG in the cells was measured by flow cytometry (Becton Dickinson), and the results were analyzed with FlowJo software (Becton Dickinson).

Fpg-sensitive qPCR

The measurement of mtDNA oxidative damage with formamidopyrimidine DNA glycosylase (Fpg)-sensitive qPCR analysis was performed according to previously reported methods [42]. In brief, 250 ng of purified mtDNA was incubated with 8 units of Fpg in 1X NEBuffer 1 and 100 mg/mL BSA in 50 mL at 37 °C for 1 h. After inactivation of the Fpg enzyme by incubation at 60 °C for 5 min, 10 ng of DNA was used for qPCR to detect Fpg-sensitive cleavage sites. Data were calculated as the quotient of signal intensities in Fpg-treated DNA relative to Fpg-untreated DNA that reflects the fraction of intact DNA.

Mitophagy measurement

Mitophagy was assessed with a mitophagy detection kit following the manufacturer's protocol (Dojindo). In brief, the cells were incubated with the mitophagy component dye (100 nmol/L) for 1 h at 37 °C. The cells were washed and then incubated with Lyso dye (1 μmol/L) for 1 h, and the fluorescence intensity of the mitophagy dye-stained mitochondria gated from positive Lyso dye-labeled lysosomes was measured via flow cytometry (Becton Dickinson).

Caspase 1 activity assay

The activity of caspase 1 was evaluated according to the instructions provided with the FAM FLICA Caspase 1 Assay Kit (Molecular Probes). After treatment, the cells were collected and washed with PBS twice. The cell pellet was subsequently resuspended in 100 μl of medium and incubated with a 30×FLICA solution (3.3 μl/sample) for 60 min at 37 °C in the dark. After being washed with washing buffer (provided with the kit), the cells were subsequently resuspended in 1 ml of washing buffer for further flow cytometry and FlowJo analysis [40].

Lactate dehydrogenase release assay

Lactate dehydrogenase (LDH) release was detected with a Cytotoxicity LDH Assay Kit (CK12, Dojindo Laboratory, Kumamoto, Japan) to measure the extent of cellular injury. The cells were seeded overnight in 96-well plates. After this, 100 μL of culture supernatant from each well was added to 100 μL of working solution and incubated for 30 min in the dark at room temperature. After adding 50 μL of stop solution, the absorbance was measured at 490 nm with a microplate reader [34].

Determination of 8-OHdG levels by flow cytometry

For intracellular 8-OHdG detection, the cells were washed twice with PBS and detached with trypsin. After fixation with 4% paraformaldehyde, the cells were permeabilized with 0.05% Triton X-100 and then blocked with PBS supplemented with 1% BSA. Goat anti-human 8-OHdG Abs (Millipore) were added and incubated for 1 h at room temperature. After washing twice with PBS, donkey anti-goat Alexa Fluor™ 488 was added, and the mixture was incubated for 0.5 h at room temperature. After additional washes with PBS, the samples were analyzed by flow cytometry [36].

Statistical analysis

All analyses were performed with a minimum of triplicates. Data from pooled donor samples are expressed as the means ± SEMs. Statistical comparisons were performed with Student's *t* test or one-way analysis of variance (ANOVA). When ANOVA revealed significant differences between groups, Bonferroni post hoc correction was performed to determine the specific pairs of groups that significantly differed. For multiple comparisons, two-way ANOVA with Holm–Sidak multiple comparisons was used for results with a normal distribution. For correlations between gene expression in clinical samples, statistical analysis was performed with the Mann–Whitney U test and the Pearson correlation coefficient. A P value <0.05 was considered to indicate statistical significance. Asterisks indicate values that are significantly different from the relevant control ($^{*}P<0.05$, $^{**}P<0.01$, $^{***}P<0.001$ and $^{****}P<0.0001$).

Results

Induction of LY6E in peripheral blood monocytes and kidney macrophages from both human and mouse systems

Induction of *LY6E* mRNA could be readily detected in monocytes collected from patients with SLE (Fig. 1A). The expression of *LY6E* correlated with that of *IFN-α1*

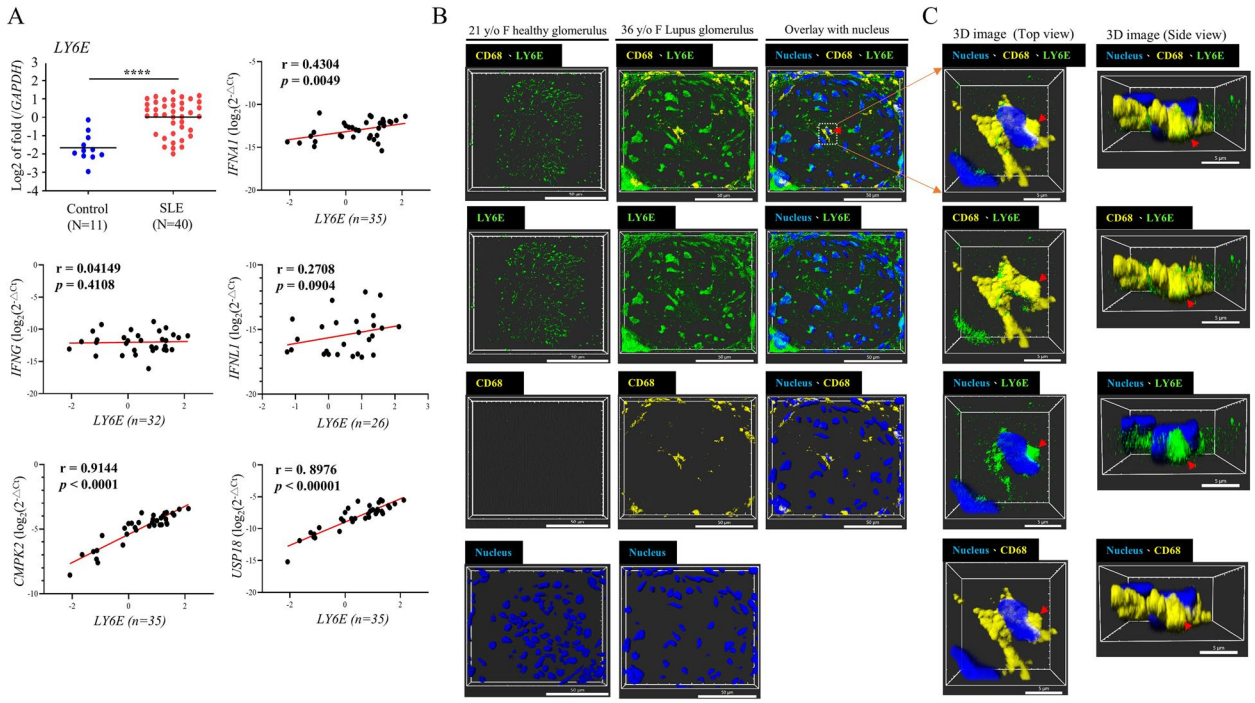

Fig. 1 Induction of LY6E in peripheral blood monocytes and kidney macrophages from SLE patients. CD14 + monocytes were prepared from the peripheral blood of 40 SLE patients and 11 healthy controls. The expression of *LY6E*, *IFNA1*, *IFNG*, *IFNL1*, *CMPK2 and USP18* mRNAs was determined by qPCR and analyzed via the Mann–Whitney U test and Pearson correlation coefficient. Each data point represents a log2 ($2^{-\Delta.Ct}$) value for *LY6E* in an individual patient (**A**). The correlations between *LY6E* mRNA and *IFNA1*, *IFNG*, *IFNL1*, *CMPK2 and USP18* mRNAs in CD14 + monocytes prepared from patients with SLE were analyzed (**A**). Kidney samples from a 21-year-old healthy female and a 36-year-old female patient with lupus nephritis were examined by immunohistochemical staining and analyzed by confocal microscopy, and 3-dimensional (**B**) and 3-dimensional zoomed-in images (**C**) are shown. ****$P < 0.0001$

but not that of *IFN-γ* or *IFN-λ1* (*IFN-γ* and *IFN-λ1* were undetectable in some samples) and correlated with the expression of IFN-stimulated genes such as *CMPK2* and *USP18* (Fig. 1A), whose immunomodulatory roles in SLE have been investigated in this laboratory [34, 37]. The demographic information about the studied SLE patients and controls is presented in Supplementary Table 3 of our previous report [34]. To determine the expression of LY6E in human samples, we purchased kidney samples of a 21-year-old healthy individual and a 36-year-old lupus nephritis patient and performed immunohistochemical staining analysis. As shown in the 3-dimensional images, increased numbers of macrophages and higher expression of LY6E were observed in the kidney samples from a patient with lupus nephritis than in those from a healthy individual, where weak LY6E expression could be detected in various renal resident cells (Fig. 1B). Colocalization of the macrophage marker CD68 and LY6E was evident in zoomed-in 3-dimensional images from the confocal microscopic examination (Fig. 1C). The increased expression of LY6E was not limited to macrophages and non-macrophage immune cells and renal resident cells such as endothelial cells, podocytes, mesangial cells, and epithelial cells might also contribute to the increased LY6E + signals in both glomerulus and interstitium (Fig. 1C and Supplementary Fig. 1). Because these non-macrophage immune cells or non-immune cells were not specifically labeled and studied, the significance of LY6E induction in these cells is currently unclear. To further investigate the significance and mechanisms of LY6E induction in monocytes and macrophages of SLE patients, we chose to study a mouse system. In pristane-induced lupus-prone (PIL) mice, increased serum antinuclear antibody (ANA) levels (Fig. 2A), enlarged spleens (Fig. 2B) and prominent inflammatory cell infiltration in the kidneys (Fig. 2C) were observed. Similar to that observed in the human system, increased LY6E expression and the colocalization of LY6E and the murine macrophage marker F4/80 in the glomerulus and the interstitium were observed in 3-dimensional images from confocal microscopy (Fig. 2D and 2E and Supplementary Fig. 2). Notably, there was a significantly greater number of LY6E-positive macrophages than LY6E-negative macrophages in the kidneys of PIL mice (Fig. 2F).

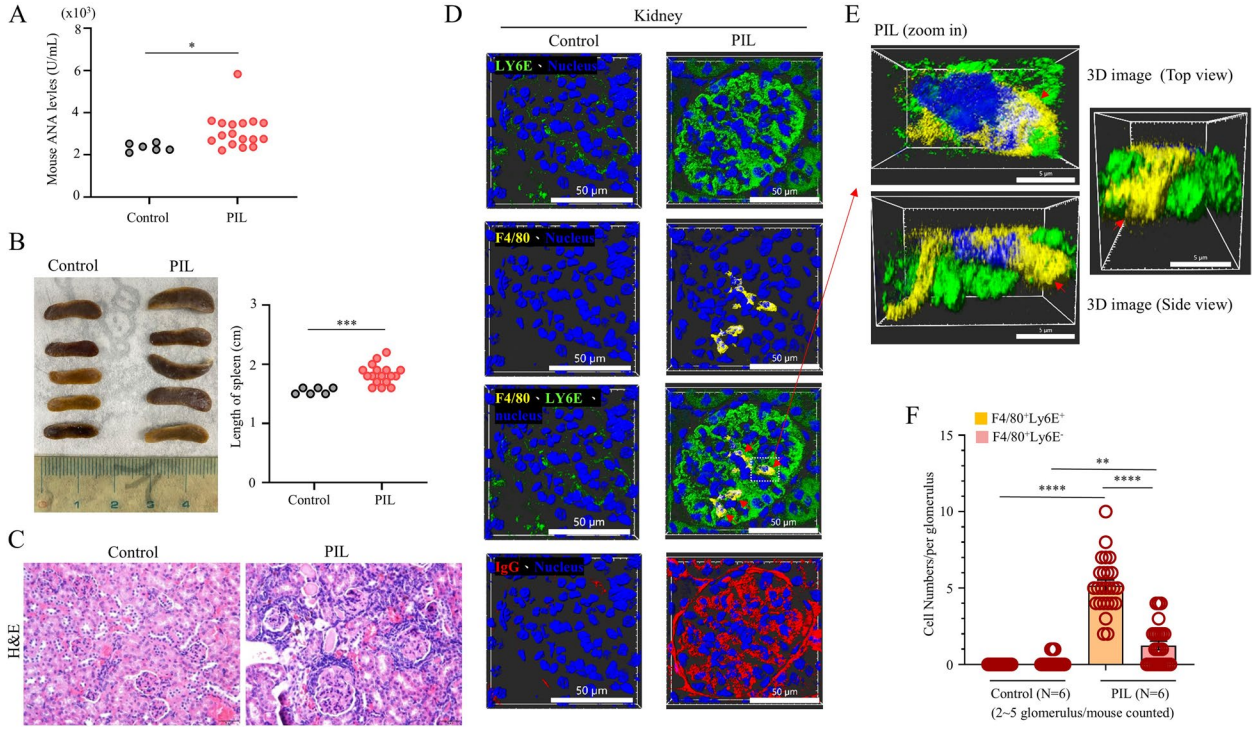

Fig. 2 There was a greater population of infiltrating macrophages in kidneys that expressed LY6E compared to those not expressing LY6E in pristane-induced lupus mice. Various numbers of pristane-induced lupus-prone mice were generated as described, maintained for 7 months and then sacrificed for the indicated studies. Several parameters related to inflammation were subsequently analyzed. The titers of serum ANA (**A**), sizes of the spleens (**B**), and H&E stains of the kidneys (**C**) were assessed in different tissue samples from PIL mice and control mice. The results of the immunohistochemical staining analysis of kidneys stained with Abs against LY6E (green), the mouse macrophage marker F4/80 (yellow), and IgG (red) and analyzed by confocal microscopy are presented in 3-dimensional (**D**) and 3-dimensional zoomed-in (**E**) images. The number of macrophages that expressed LY6E (LY6E+) or not (LY6E-) was calculated from 2–5 glomeruli of individual mice (**F**). Statistical analysis was performed with an unpaired t test and two-way ANOVA with Holm–Sidak's multiple comparisons test to compare differences among different treatments. **P* < 0.05, ***P* < 0.01, ****i < 0.0001. PIL, pristane-induced lupus

LY6E regulated IL-1β production

The immunomodulatory effects and mechanisms of LY6E were examined in BMDMs. We found that many potential immunopathogenic triggers of SLE, such as LPS, proinflammatory cytokines, and TLR7 agonists, could induce *Ly6e* mRNA expression in BMDMs (Supplementary Fig. 3). To investigate the roles of LY6E, both the mRNA and protein levels were attenuated by introducing LY6E small interfering RNA (siRNA) into BMDMs (Fig. 3A and B). Under LY6E deficiency conditions, the expression of several inflammation-associated molecules, including proinflammatory cytokines and adhesion molecules, induced by different lupus-associated immunopathogenic signals, including IFN-α, immune complexes (ICs), lipopolysaccharide (LPS), the TLR7/8 agonist R848 and the TLR3 agonist PolyIC, was differentially regulated (Fig. 3C). Given that IL-1 plays critical roles in the immunopathogenesis of lupus-prone mice and that IFN-α and IC deposition play crucial pathogenic roles in human lupus [17, 18], we focused on investigating the roles of LY6E in IFN-α- and IC-induced IL-1β. Using Western blot analysis, we confirmed that LY6E knockdown inhibited IFN-α- and IC-induced IL-1β protein production (Fig. 3D and E).

LY6E regulated the IFN-α- and IC-induced secretion of mature IL-1β and foam cell formation

IL-1β is generated as a pro-IL-1β protein that, after enzyme digestion, is converted to mature IL-1β (mIL-1β), which is secreted by cells. We found that stimulation with IFN-α but not LPS alone increased mIL-1β levels in both total cell lysates and supernatants, and the effect was further enhanced by the addition of LPS but suppressed under LY6E deficiency conditions (Fig. 4A). BMDMs stimulated with LPS + nigericin served as a positive control. Statistical analysis of several independent experiments confirmed these results (Fig. 4B). Similarly, treatment with ICs increased mIL-1β production and secretion, and these effects were decreased by LY6E knockdown

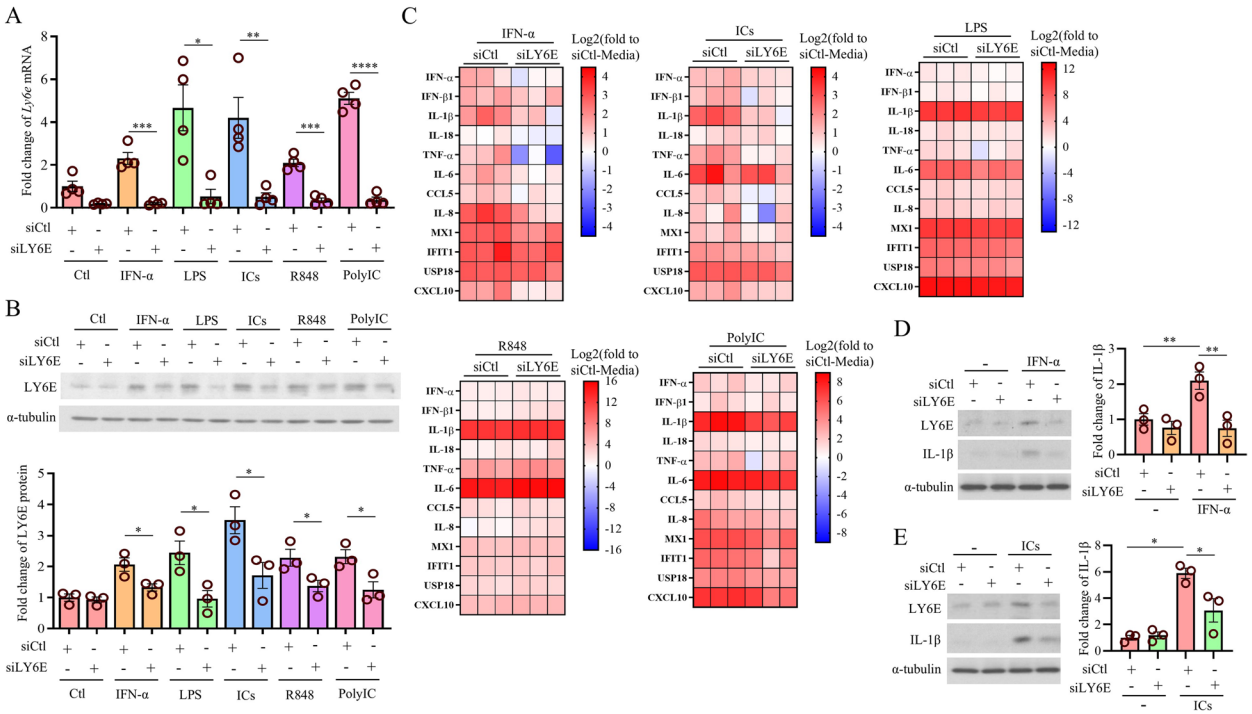

Fig. 3 LY6E deficiency inhibited IL-1β expression induced by stimulation with IFN-α and ICs. BMDMs ($2\times10.^{6}$) were electroporated with 300 nM LY6E siRNA (siLY6E) or control siRNA (siCtl) and then stimulated with or without various stimuli as indicated for 24 h. The concentrations of the individual stimuli used were as follows: the TLR7/8 agonist R848 (2.5 μg/ml), the TLR3 agonist PolyIC (10 μg/ml), LPS (100 ng/ml), IFN-α (100 U/ml), and ICs (10 μg/ml). The mRNA and protein levels of LY6E were determined by qPCR (**A**) and Western blotting (**B**), respectively. The mRNA expression of several inflammation-associated molecules induced by various stimuli with or without LY6E deficiency conditions was determined (**C**). The IFN-α- and IC-induced expression of IL-1β with or without LY6E knockdown was determined by Western blotting (**D** and **E**). Each data point represents one mouse, and the values are fold changes relative to the mean of the siCtl in RT–qPCR and Western blotting. For Western blotting, the samples were derived from the same experiment, and both the gels and the blots were processed in parallel. Statistical analysis was performed with Student's t test to compare the means between two groups (A and B) or two-way ANOVA with Holm–Sidak's multiple comparisons test to compare differences among different treatments (**D** and **E**). *$P<0.05$, **$P<0.01$, ****$P<0.0001$

(Fig. 4C and D). Although stimulation with IFN-α or ICs alone did not evidently affect the levels of pro-IL-1β, both stimuli significantly increased the total amount of IL-1β (pro-IL-1β plus mIL-1β) in BMDMs (Supplementary Fig. 4A and 4B). Given the important roles of IL-1 in foam cell formation [43] and potentially in SLE-accelerated atherosclerosis, we examined the effects of LY6E deficiency on foam cell formation. We showed that after background treatment with oxidized LDL (oxLDL), the enhanced foam cell formation induced by IFN-α or ICs was suppressed by LY6E knockdown (Fig. 4E, F, 4G and 4H). Analysis with BODIPY dye revealed results consistent with those from the Oil Red O staining (4I and 4 J). To study the mechanisms responsible for mIL-1β production and secretion, we measured the expression of active caspase 1, an enzyme mediating the cleavage of pro-IL-1β to mIL-1β, and observed that LY6E knockdown inhibited the IFN-α-, IC-, and LPS + nigericin-induced expression of caspase 1 by flow cytometry (Fig. 5A, B and C) and active caspase 1 protein production by Western blotting (Fig. 5D, E and F). LY6E knockdown inhibited IFN-α- and IC-induced NLRP3 expression (Fig. 5G and H). A positive correlation between LY6E and NLRP3 was detected in monocytes from patients with SLE (Fig. 5I). Given that complement 5a receptor 1 (C5aR1) may also regulate IL-1β production [44], the results suggest that LY6E knockdown inhibited *C5ar1* mRNA expression, although the expression of *C5ar1* mRNA did not appear to be affected by IFN-α or IC stimulation (Fig. 5J). These results suggest that the inhibition of caspase 1 and C5aR1 contributed to LY6E-regulated IL-1β production.

LY6E regulated the IFN-α- and IC-induced release of mtDNA but not mtRNA

Several mechanisms have been reported to regulate IL-1β production, and we focused on the impact of mtDNA and mtRNA released into the cytosol [45]. LY6E deficiency suppressed the IFN-α- and IC-induced release of

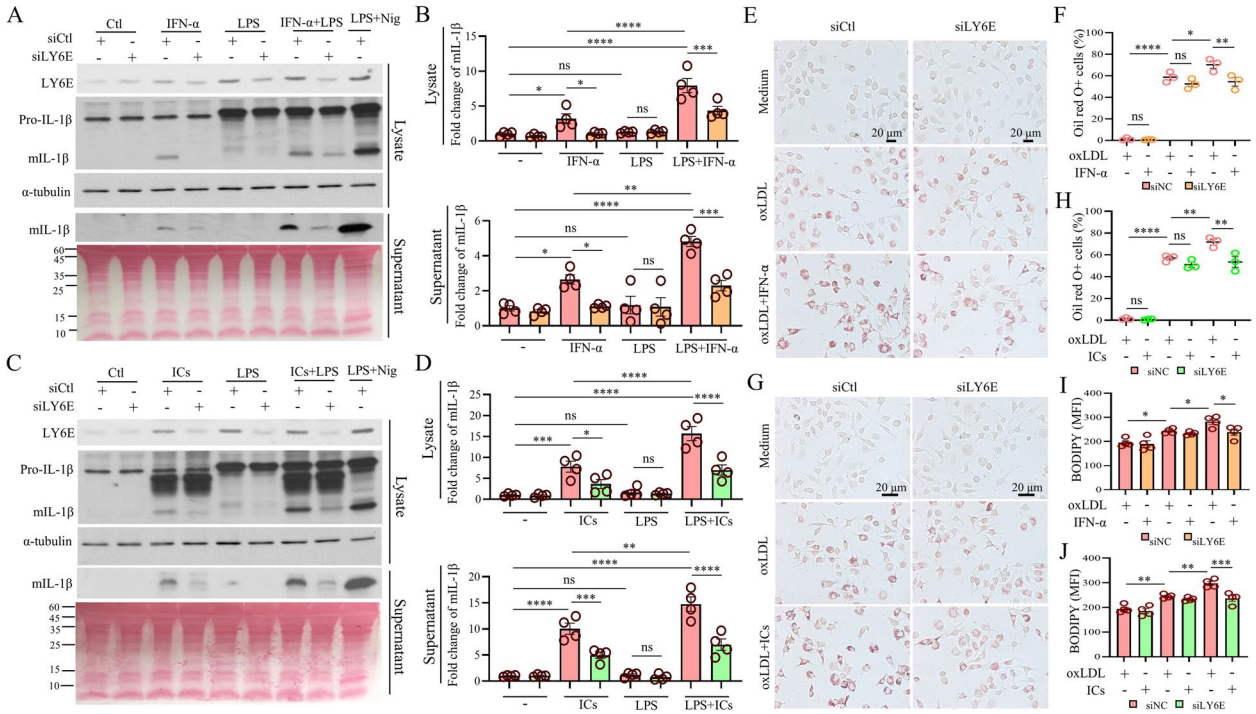

Fig. 4 LY6E deficiency inhibited mIL-1β production and foam cell formation induced by IFN-α and ICs. BMDMs (2×10^6) were electroporated with 300 nM LY6E siRNA (siLY6E) or control siRNA (siCtl) and then stimulated with or without IFN-α (100 U/ml), 10 μg/ml ICs, 100 ng/ml LPS, or a combination of these stimuli for 24 h. For inflammasome activation control, cells were stimulated with LPS (500 ng/mL) for 4 h, followed by treatment with nigericin (5 μM) for 1 h (LPS + Nig). The total cell lysates and supernatants were separately collected for the measurement of several proteins as indicated by Western blotting (**A** and **C**). The loading control for supernatants is shown with Ponceau S stain. Each data point represents one mouse, and values are fold changes relative to the mean of the siCtl group. The statistical results from several independent experiments are shown (**B** and **D**). BMDMs were stimulated with oxLDL in the presence or absence of IFN-α or ICs, and foam cell formation was measured by Oil Red O staining. The cells were examined via light microscopy, and the percentages of Oil Red O-positive cells in 5 microscopic fields for each independent experiment were determined and statistically analyzed (**E**, **F**, **G** and **H**). Moreover, BODIPY dye analysis was carried out according to the description in the Materials and Methods (**I** and **J**). Each data point represents one mouse, and the values are fold changes relative to the mean of the siCtl treatment, as determined by Western blotting. Statistical analysis was performed with two-way ANOVA with Holm–Sidak multiple comparisons to compare differences among different treatments. *$P < 0.05$, **$P < 0.01$, ***$P < 0.001$, ****$P < 0.0001$

mtDNA; however, IFN-α or IC stimulation did not affect total mtDNA (Fig. 6A). Unexpectedly, LY6E knockdown affected neither the IFN-α- nor the IC-induced release of mtRNA into the cytosol (Fig. 6B). Similarly, the activation of mtRNA downstream signaling molecules, retinoic acid-inducible gene I (RIG-I) and melanoma differentiation-associated protein 5 (MDA5), was not affected by LY6E knockdown (Fig. 6C). The mechanisms of the selective suppression of IFN-α- and IC-induced mtDNA but not mtRNA release by LY6E knockdown are currently unclear. By inhibiting IFN-α- and IC-induced mtDNA release into the cytosol, LY6E deficiency also attenuated IFN-α- and IC-induced phosphorylation and activation of STING and TANK-binding kinase 1 (TBK1) (Fig. 6D and E), both of which are important downstream signaling molecules, following the release of mtDNA into the cytosol.

LY6E regulated the generation of mitochondrial reactive oxygen species (mtROS) and oxidized mtDNA

We investigated the mechanisms by which LY6E knockdown regulates mtDNA release. We showed that LY6E knockdown inhibited the IFN-α- and IC-induced generation of mtROS (Fig. 7A) and ROS (Fig. 7B), which can affect the release of mtDNA [36]. To determine the mtDNA oxidation status, we used formamidopyrimidine DNA glycosylase (Fpg)-sensitive real-time PCR analysis [46]. As treatment of mtDNA with Fpg removes oxidized purines from the DNA and creates single-strand breaks leading to blockade of PCR amplification at these sites, the different intensities of qPCR amplification between Fpg-treated and Fpg-untreated DNA reflect oxidative base damage and the percentage of intact DNA; recognition and cleavage by Fpg causes a decrease in the

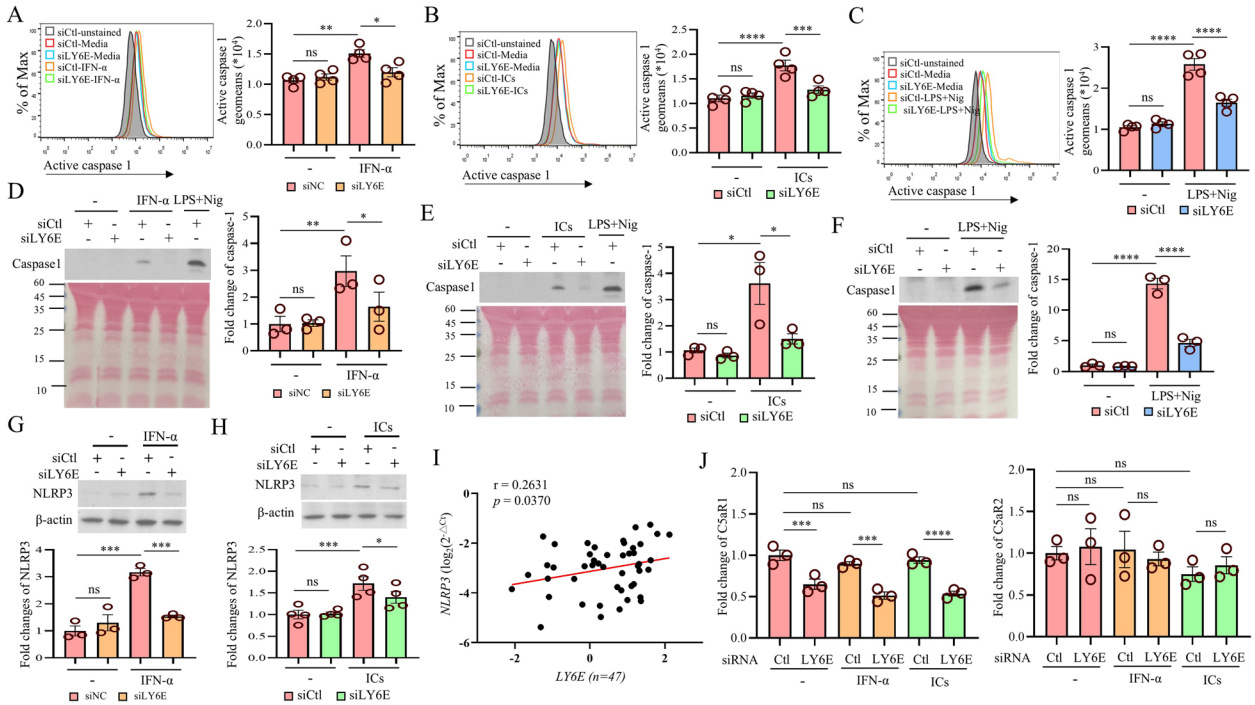

Fig. 5 LY6E knockdown inhibited the IFN-α- and IC-induced expression of active caspase 1. BMDMs ($2 \times 10.^{6}$) were electroporated with 300 nM siLY6E or siCtl and then stimulated with or without IFN-α or ICs for 24 h. As a positive control, LPS (500 ng/mL) was used to stimulate the cells for 4 h, followed by treatment with nigericin (5 μM) for 1 h (LPS + Nig). The expression of active caspase 1 was determined by flow cytometry in lysates (**A**, **B**, and **C**) or by Western blotting in supernatants (**D**, **E**, and **F**). NLRP3 expression was measured by Western blotting (**G** and **H**). The correlation between *LY6E* and *NLRP3* mRNA levels in monocytes from SLE patients was determined (**I**). In parallel, the expression of complement 5a receptor 1 (*C5ar1*) and *C5ar2* mRNAs was determined by qPCR (**J**). Each data point represents one mouse, and the values are fold changes relative to the mean value of the siCtl in RT–qPCR and Western blotting. The values for the flow cytometry results are presented as the geomeans (MFIs). Two-way ANOVA with Holm–Sidak multiple comparisons was used to compare differences among different treatments. *$P < 0.05$, **$P < 0.01$, ***$P < 0.001$, ****$P < 0.0001$

percentage and indicates an increase in the number of sequences harboring oxidized base products (Fig. 7C). By this approach, we demonstrated that IFN-α- and IC-induced mtDNA oxidation in both the mitochondrial and cytosolic fractions could be reversed by LY6E knockdown (Fig. 7D). LY6E deficiency also attenuated the IFN-α- and IC-induced generation of 8-OHdG (Fig. 7E and F). Interestingly, *Ogg1* mRNA expression was not affected by LY6E knockdown (Fig. 7G). We also found that at a concentration of 100 U/ml, IFN-α was not able to affect the mitochondrial membrane potential, and LY6E deficiency did not induce any changes (Supplementary Fig. 5A and 5B). Although stimulation with IFN-α or ICs induced mitophagy, we did not detect any effects of LY6E knockdown on IFN-α- and IC-induced mitophagy (Supplementary Fig. 5C and 5D). By measuring LDH release, we did not detect significant cytotoxic effects of LY6E knockdown under IFN-α or IC stimulation (Supplementary Fig. 5E). Furthermore, several important molecules associated with mitochondrial biogenesis (e.g., TFAM, PGC1α, NRF1, NRF2, and PPARγ), mitochondrial antioxidant defense (e.g., SOD1 and SOD2), mitochondrial fusion (e.g., MFN1), and mitochondrial fission (e.g., DRP1) were not affected by LY6E knockdown (Supplementary Fig. 6).

Reproduction of LY6E knockdown-mediated effects with inhibitors

We then used alternative approaches to determine whether these observed effects of LY6E knockdown could be reproduced by studying the effects of specific inhibitors of these signaling pathways. We showed that treatments with cyclosporin A (CsA) and a voltage-dependent anion channel oligomerization inhibitor (VBIT-4) (both block the release of mtDNA), MitoTempo (a specific scavenger of mitochondrial superoxide), H151 (a STING-specific inhibitor), and YVAD peptides (which inhibit caspase 1) all significantly suppressed IFN-α-induced mIL-1β production (Fig. 8A, C, E and G, respectively) and IC-induced mIL-1β production (Fig. 8B, D, F, and H, respectively). These results confirm the effects of LY6E knockdown on IFN-α- and IC-induced IL-1β production.

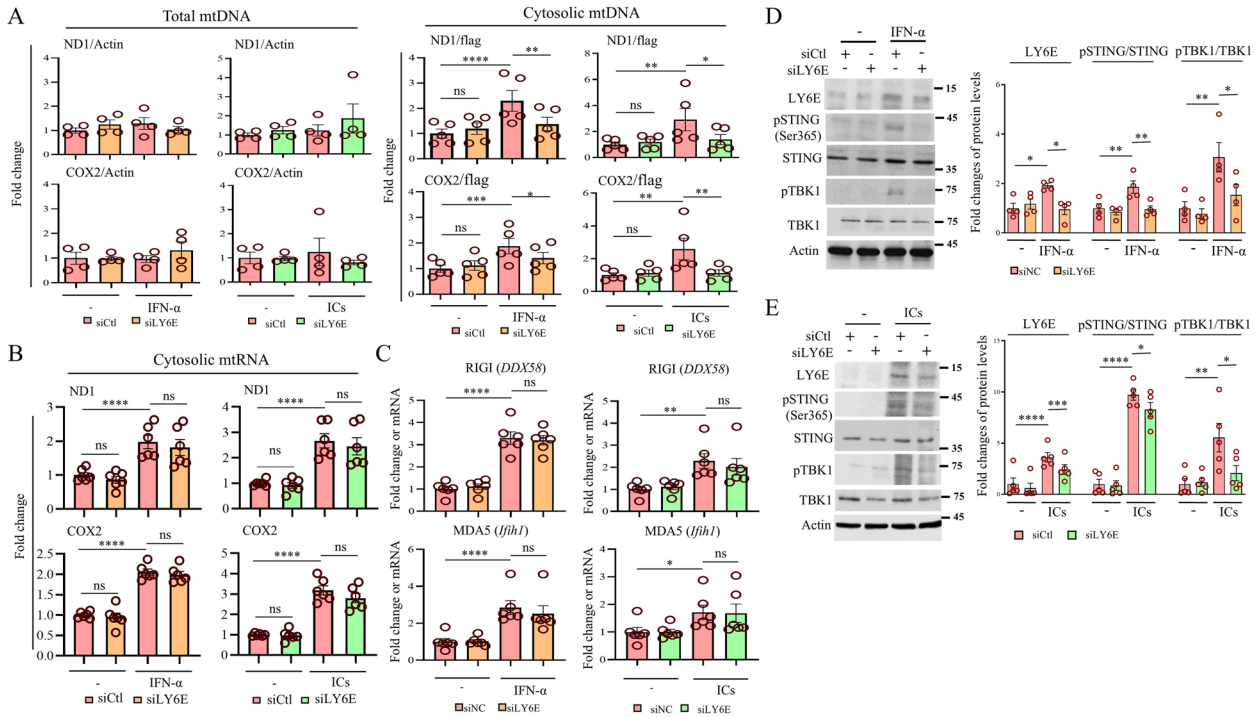

Fig. 6 LY6E regulated the IFN-α- and IC-induced release of mtDNA into the cytosol. BMDMs were electroporated with siLY6E or siCtl and then stimulated with or without IFN-α or ICs for 24 h. Both total DNA and cytosolic DNA were extracted to measure mtDNA levels with specific primers via qPCR, as described in the Materials and Methods. The relative abundance of total and cytosolic mtDNA was determined by normalization to actin or an exogenously added plasmid encoding the FLAG gene (PCR3.1-flag) (**A**). The levels of cytosolic mtRNA were similarly measured (**B**). The expression of two mtRNA downstream signaling molecules, RIG-1 and MDA5, was determined by qPCR (**C**). Several mtDNA downstream signaling molecules, such as STING and TBK1, were examined for their activation status in IFN-α-stimulated (**D**) and IC-stimulated (**E**) BMDMs by Western blotting. For Western blotting, the samples were derived from the same experiment, and both the gels and the blots were processed in parallel. Each data point represents one mouse, and the values are fold changes relative to the mean value of the siCtl in RT–qPCR and Western blotting. Two-way ANOVA with Holm–Sidak multiple comparisons was used to compare differences among different treatments. *$P < 0.05$, **$P < 0.01$, ***$P < 0.001$, ****$P < 0.0001$

LY6E was an upstream regulator of the mitochondrial molecule CMPK2

We wondered whether the LY6E-mediated effects on mtDNA release and mitochondria-associated mechanisms occurred by affecting molecules residing in mitochondria. One potentially targeted molecule is CMPK2, which resides in mitochondria and can regulate mtDNA release, as demonstrated in our previous studies [40]. In addition, there was a positive correlation between the expression of LY6E and CMPK2 in the monocytes of SLE patients (Fig. 1A). The results demonstrated that LY6E knockdown suppressed the IFN-α- and IC-induced expression of *Cmpk2* mRNA (Fig. 9A) and CMPK2 protein (Fig. 9B). Consistent with these findings, CMPK2 knockdown suppressed IFN-α- and IC-induced mIL-1β secretion and active caspase 1 expression (Fig. 9C and D). CMPK2 deficiency also inhibited LPS + nigericin-induced active capase 1 expression and mIL-1β secretion (data not shown). In contrast, LY6E levels were not affected by CMPK2 knockdown (Fig. 9C, D and Supplementary Fig. 7). Consistent with the hypothesis that CMPK2 is downstream of LY6E in the IFN-α- and IC-triggered signaling pathway, CMPK2 overexpression reversed LY6E-mediated suppression of the IFN-α- and IC-induced secretion of mIL-1β (Fig. 9E, F, and Supplementary Fig. 8A, 8B), the release of mtDNA into the cytosol (Fig. 9G and H), the activation of caspase 1, and mtROS production (Supplementary Fig. 8C and 8D). Because we could not detect LY6E in the mitochondrial compartment under both resting and IFN-α- or IC-stimulated conditions (Supplementary Fig. 9), the results suggest that LY6E might directly mediate its effects through transcriptionally regulating CMPK2 expression, which accounted for several effects observed in LY6E-knockdown cells. Given that CMPK2 is downstream of STAT1 [40], we demonstrated that LY6E knockdown also inhibited IFN-α- and IC-induced STAT1 phosphorylation (Supplementary Fig. 10).

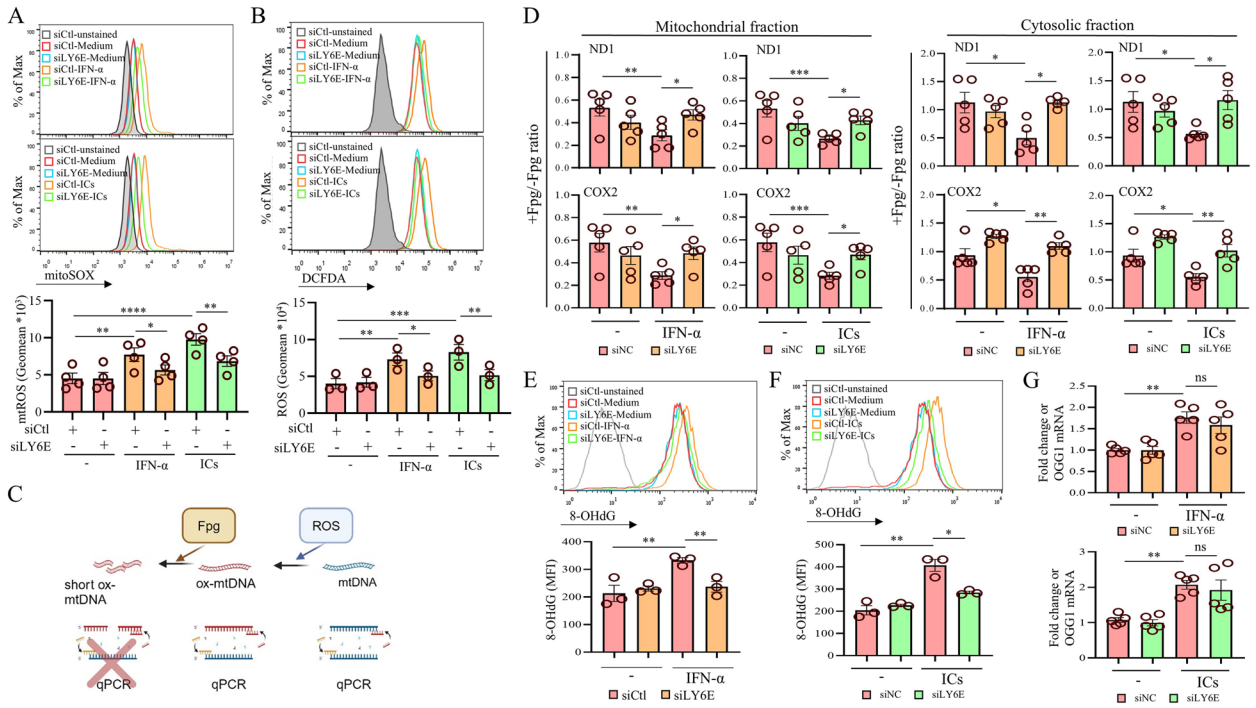

Fig. 7 LY6E inhibited the production of mtROS, ROS, oxidized mtDNA and 8-OHdG but not OGG-1 induced by IFN-α and IC stimulation. BMDMs were electroporated with siLY6E or siCtl and then stimulated with or without IFN-α or ICs for 24 h. After adding 5 μM MitoSOX™ to the culture and incubating for 0.5 h, the intensity of MitoSOX fluorescence was measured and used as an indicator of mtROS levels (**A**). The generation of cellular ROS was measured by DCFDA staining followed by flow cytometry analysis (**B**). To determine the status of mtDNA oxidation, we used formamidopyrimidine DNA glycosylase (Fpg)-sensitive real-time PCR analysis. Treatment of mtDNA with Fpg removes oxidized purines from DNA and creates single-strand breaks, leading to blockade of PCR amplification at these sites. The different intensities of qPCR amplification between Fpg-treated and Fpg-untreated DNA reflect oxidative base damage and the percentage of intact DNA; recognition and cleavage by Fpg causes a decrease in the percentage and indicates an increase in the number of sequences harboring oxidized base products (**C**). Accordingly, the mtDNA oxidation status was measured in both the mitochondrial and cytosolic fractions of IFN-α- and IC-treated BMDMs with or without LY6E knockdown (**D**). The generation of 8-OHdG was determined by flow cytometry (**E** and **F**). The expression of *Ogg1* mRNA was determined by qPCR (**G**). Each data point represents one mouse, and the values are fold changes relative to the mean value of the siCtl in RT–qPCR and Western blotting. The values for the flow cytometry results are presented as the geomeans (MFIs). Statistical analysis was performed with two-way ANOVA with Holm–Sidak multiple comparisons to compare differences among different treatments. *, $P < 0.05$; **, $P < 0.01$; ***, $P < 0.001$ and ****, $P < 0.0001$. MFI, mean fluorescence intensity

Synergistic effects between IL-1β and IFN-α or IL-1β and ICs in inducing ISGs expression

Because immune responses are tightly regulated by interactions among different cytokines, the possible coordinated effects of IL-1β and IFN-α or ICs were examined. The results shown in Fig. 10A demonstrated the synergistic effects of inducing the expression of several interferon-stimulated genes (ISGs), including *Mx1*, *Rsad2*, *Cxcl10*, *Usp18* and *Ifit1*, by a combination of IL-1β and IFN-α. Synergistic effects between IL-1β and ICs were also observed in the regulation of the expression of ISGs such as *Mx1*, *Rsad2*, *Cxcl10*, *Usp18* and *Ifit1* (Fig. 10B). The mechanisms by which LY6E regulates IFN-α- and IC-mediated mIL-1β production in macrophages are summarized in Fig. 11.

Discussion

In addition to the proinflammatory impact of IFN-α, the deposition of ICs in kidneys is another major contributor to lupus nephritis. Among infiltrating immune cells and resident cells in the kidney, monocytes/macrophages are critical sentinels preserving IgG-binding Fcγ receptors, the major IC responders and one of the critical cell populations in the pathogenesis of lupus nephritis [1, 6, 47, 48]. The induction of LY6E by IFN-α and ICs in BMDMs was comparable with the increased expression of LY6E in infiltrating macrophages in the kidneys of pristane-induced lupus-prone mice and patients with lupus nephritis. LY6E knockdown suppressed foam cell formation and the cellular lipid content induced by IFN-α and ICs in BMDMs, suggesting a wider role for LY6E in

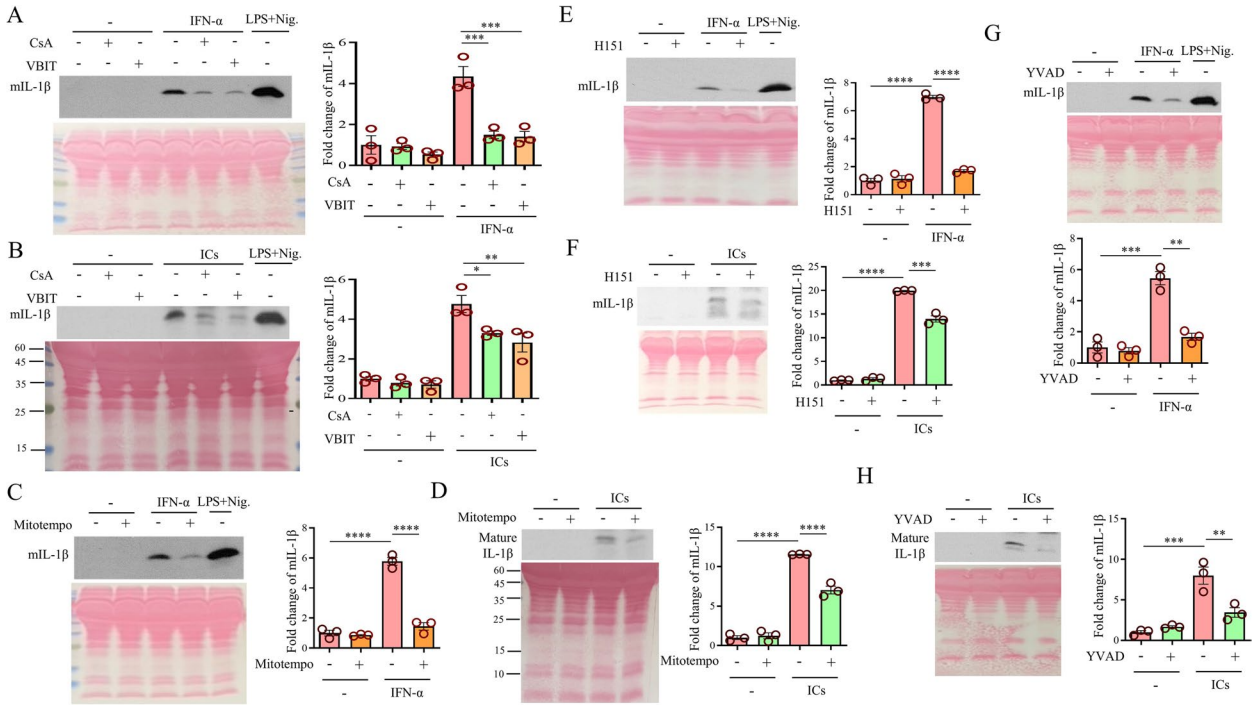

Fig. 8 LY6E-knockdown effects were reproduced with the use of specific inhibitors of several different signaling pathways. BMDMs were treated with different inhibitors targeting LY6E-regulated and IFN-α- and IC-activated downstream signaling pathways, including 5 μM CsA or 10 μM VBIT-4 (**A** and **B**), 100 μM MitoTempo (**C** and **D**), 40 μM YVAD (**G** and **H**), or 2 μg/ml H151 (**E** and **F**), for 2 h, followed by stimulation with IFN-α or ICs for 24 h (**A**, **B**, **C**, **D**, **G** and **H**) or 6 h (**E** and **F**). After that, the supernatants were collected for the measurement of mIL-1β by Western blotting. The samples were derived from the same experiment, and both the gels and the blots were processed in parallel. The results of the statistical analysis of several independent experiments are presented. Statistical analysis was performed with two-way ANOVA with Holm–Sidak multiple comparisons to compare differences among different treatments. CsA, cyclosporin A; VBIT-4, voltage-dependent anion channel oligomerization inhibitor. *, $P < 0.05$; **, $P < 0.01$; ***, $P < 0.001$ and ****, $P < 0.0001$

SLE and SLE-accelerated atherosclerosis. LY6E-mediated immunomodulation involved mitochondrial machineries such as increased mtDNA release into the cytosol, the generation of mtROS and ROS, the activation of STING and the participation of caspase 1 and NLRP3, leading to the release of mIL-1β in IFN-α- and IC-treated BMDMs. Importantly, the LY6E knockdown-mediated effect on mIL-1β production could be faithfully reproduced by chemical compounds targeting these signaling pathways. Unexpectedly, given that treatment with either IFN-α or ICs effectively induced the release of mtDNA and mtRNA from mitochondria into the cytosol, LY6E deficiency affected only mtDNA but not mtRNA release. This suggestion was supported by examining the mRNA expression of downstream signaling molecules, including RIG-1 and MDA5. Thus, the mechanisms responsible for mtDNA and mtRNA release from mitochondria to the cytosol are likely independent and differentially regulated. We currently do not know the mechanisms accounting for such a difference. Because the regulation of mtDNA and mtRNA release from mitochondria to the cytosol remains unclear, targeting LY6E may serve as a powerful tool for associated studies.

Cytokines are known to work synergistically or antagonistically to regulate immune responses during infection, inflammation and cancer. In addition, many cytokines function in an autocrine manner to regulate immune responses. Synergistic effects have also been observed between TNF and IFN in inducing the expression of ISGs through triggering interferon regulatory factor 1 (IRF1)-dependent signaling pathways [49]. In the present study, we found synergistic effects between IL-1β and IFN-α or a combination of both IL-1β and ICs in inducing the expression of several ISGs. Furthermore, our results suggest that synergistic effects on mIL-1β production occurred when BMDMs were cotreated with the pathogen-associated molecular pattern LPS and IFN-α or ICs. Given that several mechanisms were responsible for LY6E-mediated effects on IFN-α- and IC-induced mIL-1β production, it is interesting that many of these signaling events can also be activated by IL-1β stimulation. Aarreberg et al. reported that exogenous IL-1β

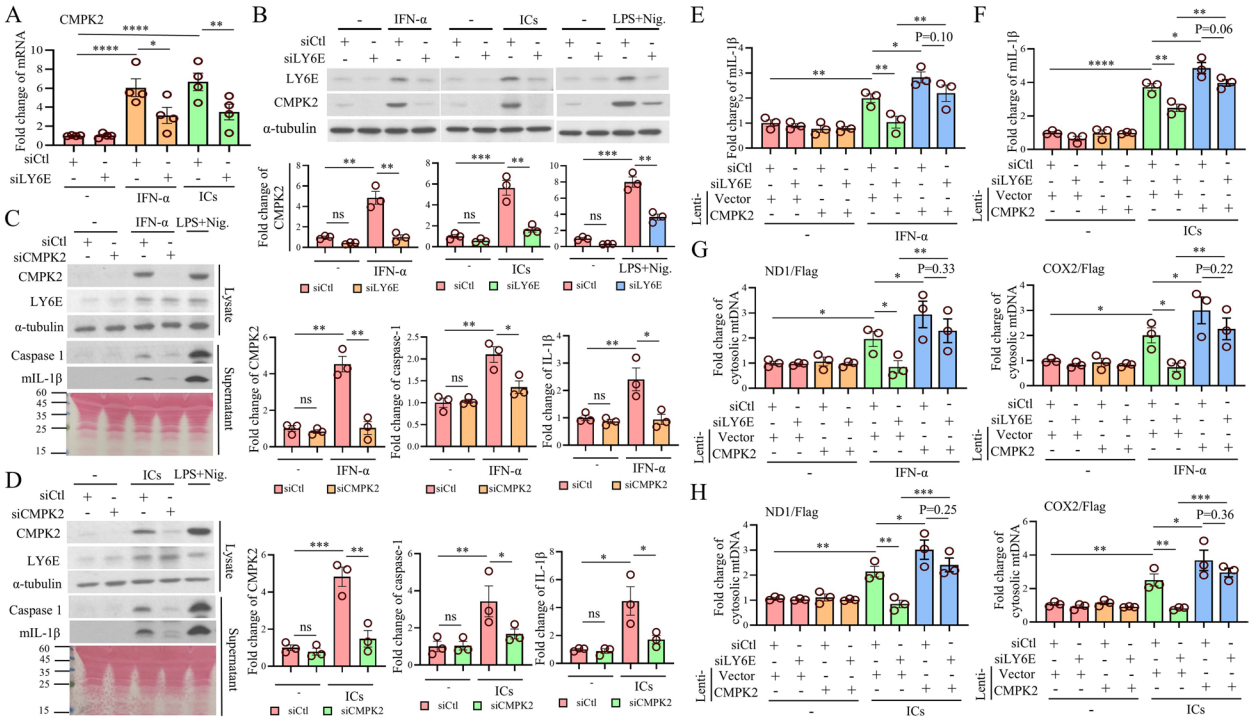

Fig. 9 LY6E mediated its effects through regulating CMPK2. BMDMs were electroporated with siLY6E or siCtl and then stimulated with or without IFN-α, ICs, or LPS + nigericin (LPS + Nig) for 24 h, after which the *Cmpk2* mRNA and protein levels were determined (**A** and **B**). BMDMs were electroporated with 300 nM siCMPK2 or siCtl and then stimulated with and without IFN-α or ICs for 24 h, and the levels of CMPK2 and LY6E in total cell lysates and both active caspase 1 (p20) and mIL-1β in supernatants were measured by Western blotting (**C** and **D**). BMDMs electroporated with siLY6E or siCtl were transduced with lentivirus carrying wild-type CMPK2-DYK or the control DYK vector. After 48 h, the medium was replaced with fresh medium, and the cells were then stimulated with IFN-α or ICs for 24 h. The measurement of mIL-1β in the supernatants (**E** and **F**) and mtDNA release into the cytosol (G and H) were carried out accordingly as previously described. Statistical analysis was performed with two-way ANOVA with Holm–Sidak multiple comparisons to compare differences among different treatments. *, $P < 0.05$; **, $P < 0.01$; ***, $P < 0.001$ and ****, $P < 0.0001$

could cause mtDNA release, induce cGAS/STING activation and lead to protection and effective limitation of virus infection [50, 51].

We found that in addition to mtDNA and mtRNA release into the cytosol, there was no evident effect on cell death or changes in the mitochondrial membrane potential caused by treatment with IFN-α or ICs. IFN-α has been shown to affect the mitochondrial membrane potential and cause cell death in various cell types under high or very high dosages of treatment, such as 5×10^4 U/ml in proximal tubular cells [52], 3,000 U/ml in human Jurkat variant H123 [53] and 1000 U/ml in CD8 + T cells [54]. Notably, Buang et al. reported that the intensity of ISG expression in IFN-high SLE patients was comparable with that observed after treatment with a 1000 U/ml dose of IFN-α [54]. The dosages of IFN-α investigated in these studies are clearly much higher than the dosage of 100 U/ml IFN-α examined in the present study, which is presumably closer to the conditions of general SLE patients. This may explain why after treatment with 100 U/ml IFN-α, we did not detect any effect on the mitochondrial membrane potential. Our results also suggest that LY6E deficiency did not affect IFN-α- or IC-induced mitophagy. Although there are defects in monocyte function in SLE patients compared with healthy controls, the number of monocytes is increased instead of decreased in SLE patients [55–57]. Furthermore, dengue virus infection induced the release of mtDNA and subsequent activation of the TLR9 signaling pathway in human dendritic cells, and these events were not accompanied by cell death [36]. Moreover, we did not detect any changes in several genes associated with mitochondrial biogenesis, fusion, or fission in response to low-dose IFN-α (100 U/ml) or IC treatment.

CMPK2 catalyzes the phosphorylation of CMP, UMP, dCMP and dUMP by ATP to the corresponding diphosphates [58, 59]. The knockdown of LY6E inhibited IFN-α- and IC-induced CMPK2 expression but not the opposite, suggesting that LY6E was upstream of CMPK2 in the IFN-α- and IC-triggered signaling pathways. Consistent with these results, the LY6E-mediated suppression of IFN-α- and IC-induced mIL-1β production was

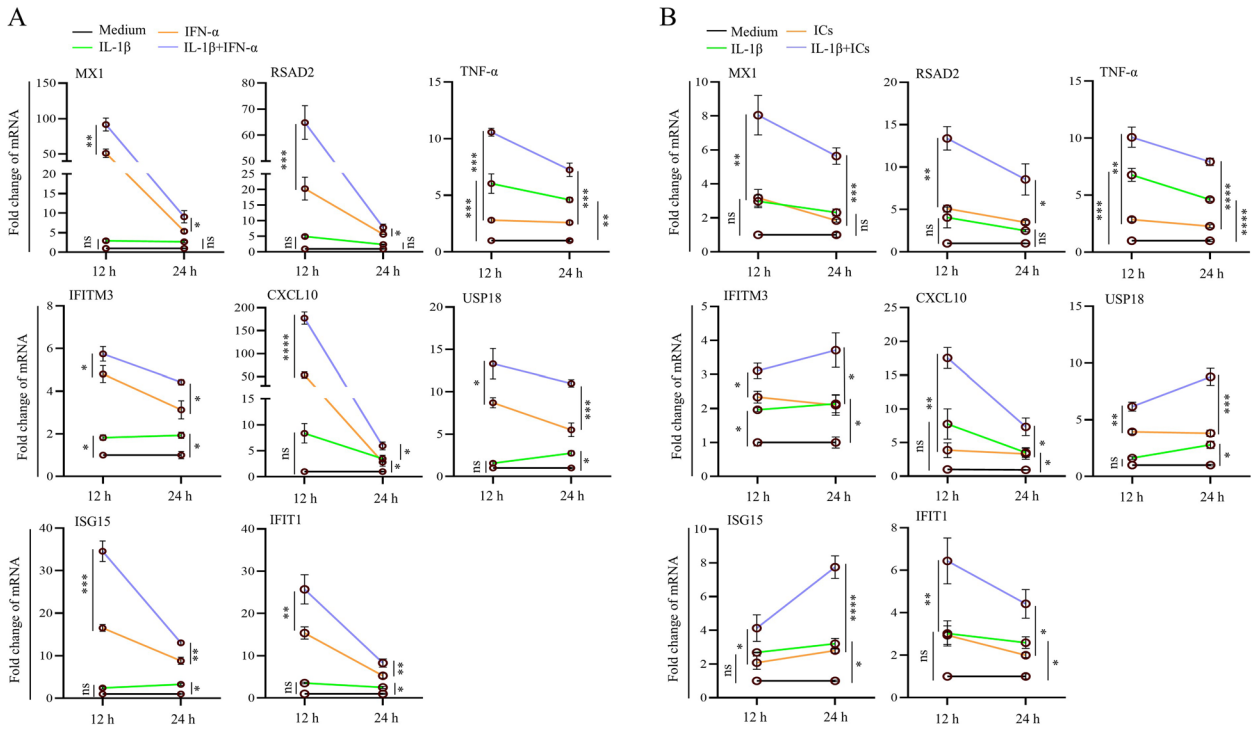

Fig. 10 Synergistic effects of a combination of IL-1β and IFN-α or IL-1β and ICs in ISGs induction. BMDMs stimulated with IL-1β, IFN-α or ICs alone or in combination for 12 h or 24 h were collected, and the expression of several ISGs as indicated was determined by qPCR. Statistical analysis was performed with two-way ANOVA with Holm–Sidak multiple comparisons to compare differences among different treatments. *, $P < 0.05$; **, $P < 0.01$; ***, $P < 0.001$ and ****, $P < 0.0001$

effectively reversed by the overexpression of CMPK2. Accordingly, the LY6E-mediated effects can be explained in part through regulating the expression of the mitochondrial protein CMPK2. CMPK2 plays crucial roles in dengue virus infection through mechanisms involving the mitochondrial machinery and downstream signaling pathways, such as the production of mtROS and ROS, the generation of 8-OHdG, mtDNA release into the cytosol, and the activation of TLR9 and the inflammasome pathway [40]. Several other events, such as cell migration, the production of cytokines such as IFN-α and IFN-λ, and foam cell formation, are also regulated by CMPK2 in macrophages [37, 40]. Importantly, although induced by IFN signaling, CMPK2 can mediate both IFN-dependent and IFN-independent mechanisms [40]. As expected, targeting LY6E may have broader immunomodulatory effects than targeting CMPK2 therapeutically.

One major limitation of our study is that most of the experiments were carried out with mouse BMDMs. Nevertheless, this limitation was partially alleviated by the results from the immunohistochemical staining analyses and confocal microscopic examinations of kidney samples from patients with lupus nephritis. Inflammatory macrophages are the dominant infiltrating immune cells in lupus nephritis [60] and contribute to the formation of tertiary lymphoid structures involved in kidney inflammation in SLE [1]. By analyzing single-cell transcriptional profiles of kidney macrophages in patients with lupus nephritis, one study identified several different subsets of macrophages that have differential abilities to take up ICs and play differential roles in the immunopathogenesis of lupus nephritis [61]. When single-cell RNA sequencing (scRNA-seq) was used to examine CD45 + immune cells, at least five myeloid subpopulations were identified in renal biopsy samples from patients with lupus nephritis in which progressive stages of monocyte differentiation within the kidney were observed [62]. We currently do not know the extent to which LY6E + macrophages in kidneys may contribute to the pathogenesis of lupus nephritis. Aside from LY6E + macrophages in glomerulus and interstitium of SLE patient's kidney samples, we also noted highly induced expression of LY6E in other cell types that may possibly include non-macrophage immune cells like T or B cells or non-immune renal resident cells although these cells were not specifically labeled and examined. In supportive, among many induced genes, the increased expression of *LY6E* mRNA has been detected in pan-T cells [63] and CD4 + T cells [64] by high depth sequencing and cell-sorted RNA-sequencing, respectively. Furthermore, positive

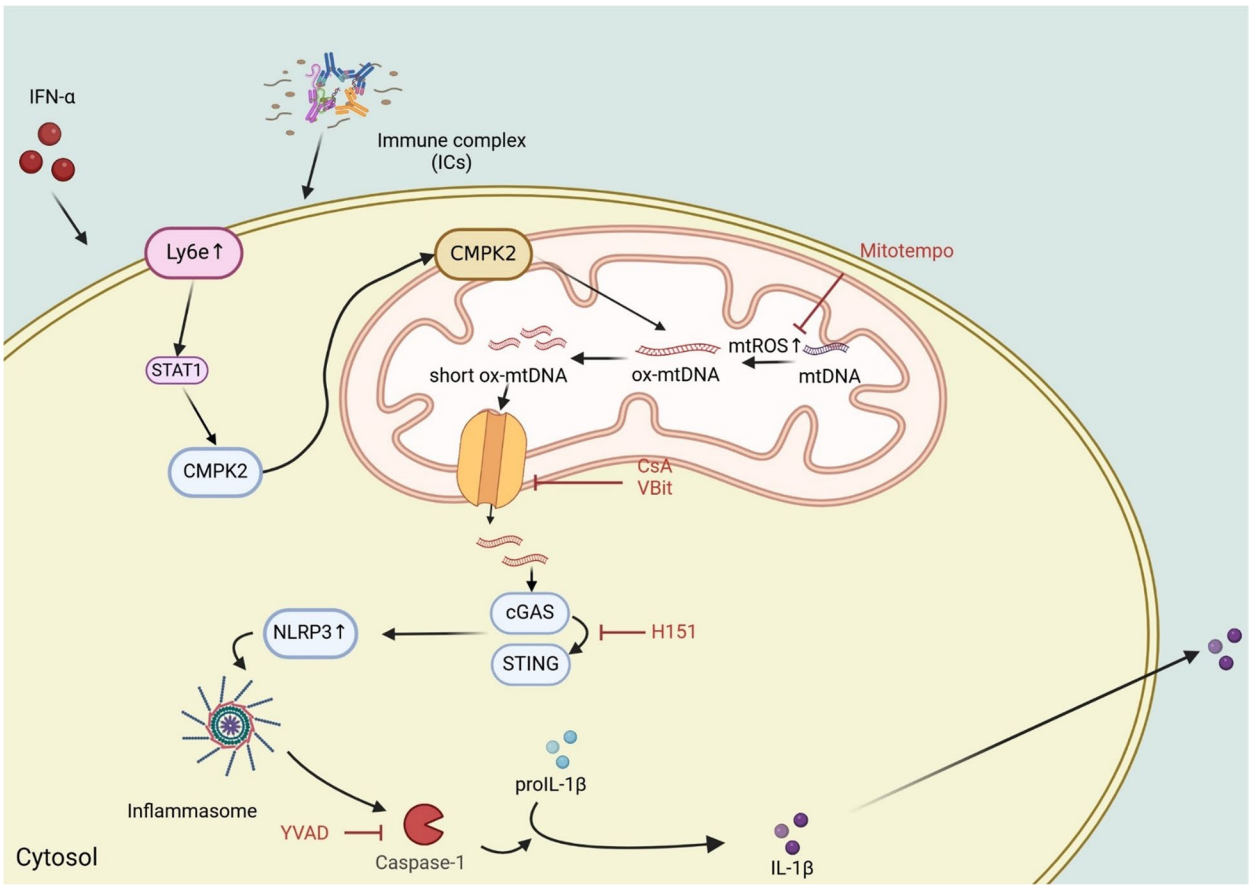

Fig. 11 The proposed model summarizes how LY6E regulates IFN-α- and IC-induced mIL-1β production. Stimulation with either IFN-α or ICs induced LY6E expression. Induction with LY6E activated STAT1 and increased the transcription of CMPK2. The translocation of CMPK2 into mitochondria is, in part, responsible for several events occurring in mitochondria, such as the generation of mtROS and ROS, the increase in oxidized mtDNA and the release of mtDNA into the cytosol. Cytosolic mtDNA then activates the cGAS/STING and TBK1 pathways and the inflammasome pathway. These events lead to an increase in mIL-1β production and secretion. Several LY6E-mediated effects can be reproduced using specific inhibitors, as indicated

correlation has been demonstrated between the ISG score measuring expression levels of LY6E and other targeted ISGs in PBMCs of SLE patients and disease activity [35], severity of lupus skin lesion [65], and therapeutic response in proliferative lupus nephritis [66]. Given the highly induced expression of LY6E in different subsets of immune and non-immune cells in lupus, targeting LY6E may be an attractive strategy for therapeutics against SLE and other autoimmune disorders.

Supplementary Information

The online version contains supplementary material available at https://doi.org/10.1186/s12964-025-02140-z.

Supplementary Material 1.

Acknowledgements
This work was supported by the Optical Biology Core Facility and the Pathology Core Laboratory of NHRI. Graphs were generated with the purchased software BioRender.

Authors' contributions
JHL and LJH conceived the study, guided the experiments, and drafted and edited the manuscript; DWW, CYH, LFH, and CHW conducted the experiments, methodology, software, and analyzed the data; JHL and LJH supervised the data analysis. SMK, AC, and JLH discussed the experiments and technique procedures throughout the studies. All the authors participated in the interpretation and discussion of the study results. All the authors read and approved the final manuscript.

Funding
The studies were supported by the Ministry of Science and Technology (NSTC 113–2314-B-182A-059-MY3 to Dr. Lai and NSTC 112–2314-B-400–012-MY2 to Dr. Ho) and Chang Gung Memorial Hospital (CMRPG1P0021), Taiwan, R.O.C.

Data availability
No datasets were generated or analysed during the current study.

Declarations

Ethics approval and consent to participate

The use of human blood samples was approved by the IRB (no. 201509825A3) of Chang Gung Memorial Hospital, Linko, Taiwan. This study was performed in accordance with the Declaration of Helsinki.

Competing interests

The authors declare no competing interests.

Author details

[1]Division of Allergy, Immunology and Rheumatology, Department of Internal Medicine, Chang Gung Memorial Hospital, Tao-Yuan, Taiwan, ROC. [2]Institute of Cellular and System Medicine, National Health Research Institute, Zhunan, Taiwan, ROC. [3]Graduate Institute of Aerospace and Undersea Medicine, Department of Medicine, National Defense Medical Center, Taipei, Taiwan, ROC. [4]Department of Pathology, Hualien Tzu Chi Hospital, Buddhist Tzu Chi Medical Foundation, Hualien, Taiwan, ROC. [5]Division of Allergy, Asthma, and Rheumatology, Department of Pediatrics, Chang Gung Memorial Hospital, Taoyuan 333, Taiwan, ROC. [6]Department of Pediatrics, New Taipei Municipal TuCheng Hospital, New Taipei City 236, Taiwan, ROC.

Received: 10 December 2024 Accepted: 6 March 2025
Published online: 20 March 2025

References

1. Tsokos GC. The immunology of systemic lupus erythematosus. Nat Immunol. 2024;25:1332–43.
2. Rahman A, Isenberg DA. Systemic lupus erythematosus. N Engl J Med. 2008;358:929–39.
3. Chen PM, Tsokos GC. Mitochondria in the Pathogenesis of Systemic Lupus Erythematosus. Curr Rheumatol Rep. 2022;24:88–95.
4. Wang L, Xu H, Yang H, Zhou J, Zhao L, Zhang F. Glucose metabolism and glycosylation link the gut microbiota to autoimmune diseases. Front Immunol. 2022;13: 952398.
5. Caielli S, Wan Z, Pascual V. Systemic Lupus Erythematosus Pathogenesis: Interferon and Beyond. Annu Rev Immunol. 2023;41:533–60.
6. Lai B, Luo SF, Lai JH. Therapeutically targeting proinflammatory type I interferons in systemic lupus erythematosus: efficacy and insufficiency with a specific focus on lupus nephritis. Front Immunol. 2024;15:1489205.
7. Felten R, Scher F, Sagez F, Chasset F, Arnaud L. Spotlight on anifrolumab and its potential for the treatment of moderate-to-severe systemic lupus erythematosus: evidence to date. Drug Des Devel Ther. 2019;13:1535–43.
8. Morand EF, Furie R, Tanaka Y, Bruce IN, Askanase AD, Richez C, Bae SC, Brohawn PZ, Pineda L, Berglind A, et al. Trial of Anifrolumab in Active Systemic Lupus Erythematosus. N Engl J Med. 2020;382:211–21.
9. Chen KJ, Zhang J, LaSala D, Basso J, Chun D, Zhou Y, McDonald PP, Perkins WR, Cipolla DC. Brensocatib, an oral, reversible inhibitor of dipeptidyl peptidase 1, mitigates interferon-alpha-accelerated lupus nephritis in mice. Front Immunol. 2023;14:1185727.
10. Krysko DV, Agostinis P, Krysko O, Garg AD, Bachert C, Lambrecht BN, Vandenabeele P. Emerging role of damage-associated molecular patterns derived from mitochondria in inflammation. Trends Immunol. 2011;32:157–64.
11. West AP, Khoury-Hanold W, Staron M, Tal MC, Pineda CM, Lang SM, Bestwick M, Duguay BA, Raimundo N, MacDuff DA, et al. Mitochondrial DNA stress primes the antiviral innate immune response. Nature. 2015;520:553–7.
12. Rongvaux A, Jackson R, Harman CC, Li T, West AP, de Zoete MR, Wu Y, Yordy B, Lakhani SA, Kuan CY, et al. Apoptotic caspases prevent the induction of type I interferons by mitochondrial DNA. Cell. 2014;159:1563–77.
13. Caielli S, Athale S, Domic B, Murat E, Chandra M, Banchereau R, Baisch J, Phelps K, Clayton S, Gong M, et al. Oxidized mitochondrial nucleoids released by neutrophils drive type I interferon production in human lupus. J Exp Med. 2016;213:697–713.
14. Caielli S, Cardenas J, de Jesus AA, Baisch J, Walters L, Blanck JP, Balasubramanian P, Stagnar C, Ohouo M, Hong S, et al. Erythroid mitochondrial retention triggers myeloid-dependent type I interferon in human SLE. Cell. 2021;184(4464–79): e19.
15. Riley JS, Tait SW. Mitochondrial DNA in inflammation and immunity. EMBO Rep. 2020;21: e49799.
16. Lemay S, Mao C, Singh AK. Cytokine gene expression in the MRL/lpr model of lupus nephritis. Kidney Int. 1996;50:85–93.
17. Boswell JM, Yui MA, Endres S, Burt DW, Kelley VE. Novel and enhanced IL-1 gene expression in autoimmune mice with lupus. J Immunol. 1988;141:118–24.
18. Voronov E, Dayan M, Zinger H, Gayvoronsky L, Lin JP, Iwakura Y, Apte RN, Mozes E. IL-1 beta-deficient mice are resistant to induction of experimental SLE. Eur Cytokine Netw. 2006;17:109–16.
19. McCarthy EM, Smith S, Lee RZ, Cunnane G, Doran MF, Donnelly S, Howard D, O'Connell P, Kearns G, Ni Gabhann J, Jefferies CA. The association of cytokines with disease activity and damage scores in systemic lupus erythematosus patients. Rheumatology (Oxford). 2014;53:1586–94.
20. Italiani P, Manca ML, Angelotti F, Melillo D, Pratesi F, Puxeddu I, Boraschi D, Migliorini P. IL-1 family cytokines and soluble receptors in systemic lupus erythematosus. Arthritis Res Ther. 2018;20:27.
21. Caielli S, Balasubramanian P, Rodriguez-Alcazar J, Balaji U, Robinson L, Wan Z, Baisch J, Smitherman C, Walters L, Sparagana P, et al. Type I IFN drives unconventional IL-1beta secretion in lupus monocytes. Immunity. 2024;57(11):2497-513e12. https://doi.org/10.1016/j.immuni.2024.09.004. https://www.ncbi.nlm.nih.gov/pubmed/39378884.
22. Kahlenberg JM, Yalavarthi S, Zhao W, Hodgin JB, Reed TJ, Tsuji NM, Kaplan MJ. An essential role of caspase 1 in the induction of murine lupus and its associated vascular damage. Arthritis Rheumatol. 2014;66:152–62.
23. Zhao J, Wang H, Dai C, Wang H, Zhang H, Huang Y, Wang S, Gaskin F, Yang N, Fu SM. P2X7 blockade attenuates murine lupus nephritis by inhibiting activation of the NLRP3/ASC/caspase 1 pathway. Arthritis Rheum. 2013;65:3176–85.
24. Bennett TD, Fluchel M, Hersh AO, Hayward KN, Hersh AL, Brogan TV, Srivastava R, Stone BL, Korgenski EK, Mundorff MB, et al. Macrophage activation syndrome in children with systemic lupus erythematosus and children with juvenile idiopathic arthritis. Arthritis Rheum. 2012;64:4135–42.
25. Dein E, Ingolia A, Connolly C, Manno R, Timlin H. Anakinra for Recurrent Fevers in Systemic Lupus Erythematosus. Cureus. 2018;10: e3782.
26. Kubler L, Bittmann I, Kuipers JG. Macrophage activation syndrome triggered by active systemic lupus erythematosus : Successful treatment by interleukin-1 inhibition (anakinra). Z Rheumatol. 2020;79:1040–5.
27. Tayer-Shifman OE, Ben-Chetrit E. Refractory macrophage activation syndrome in a patient with SLE and APLA syndrome - Successful use of PET- CT and Anakinra in its diagnosis and treatment. Mod Rheumatol. 2015;25:954https://www.ncbi.nlm.nih.gov/pubmed/390585147.
28. Baldo F, Erkens RGA, Mizuta M, Rogani G, Lucioni F, Bracaglia C, et al. Current treatment in macrophage activation syndrome worldwide: a systematic literature review to inform the METAPHOR project. Rheumatology (Oxford). 2024;64(1):32–44. https://doi.org/10.1093/rheumatology/keae391. https://www.ncbi.nlm.nih.gov/pubmed/39058514.
29. Upadhyay G. Emerging Role of Lymphocyte Antigen-6 Family of Genes in Cancer and Immune Cells. Front Immunol. 2019;10:819.
30. Lee PY, Wang JX, Parisini E, Dascher CC, Nigrovic PA. Ly6 family proteins in neutrophil biology. J Leukoc Biol. 2013;94:585–94.
31. Gumley TP, McKenzie IF, Sandrin MS. Tissue expression, structure and function of the murine Ly-6 family of molecules. Immunol Cell Biol. 1995;73:277–96.
32. Rajah MM, Bernier A, Buchrieser J, Schwartz O. The Mechanism and Consequences of SARS-CoV-2 Spike-Mediated Fusion and Syncytia Formation. J Mol Biol. 2022;434: 167280.
33. Majdoul S, Compton AA. Lessons in self-defence: inhibition of virus entry by intrinsic immunity. Nat Rev Immunol. 2022;22:339–52.
34. Lai JH, Wu DW, Huang CY, Hung LF, Wu CH, Ho LJ. USP18 induction regulates immunometabolism to attenuate M1 signal-polarized macrophages and enhance IL-4-polarized macrophages in systemic lupus erythematosus. Clin Immunol. 2024;265: 110285.
35. Feng X, Wu H, Grossman JM, Hanvivadhanakul P, FitzGerald JD, Park GS, Dong X, Chen W, Kim MH, Weng HH, et al. Association of increased interferon-inducible gene expression with disease activity and lupus nephritis in patients with systemic lupus erythematosus. Arthritis Rheum. 2006;54:2951–62.

36. Lai JH, Wang MY, Huang CY, Wu CH, Hung LF, Yang CY, et al. Infection with the dengue RNA virus activates TLR9 signaling in human dendritic cells. EMBO Rep. 2018;19(8). https://doi.org/10.15252/embr.201846182. https://www.ncbi.nlm.nih.gov/pubmed/29880709.
37. Lai JH, Hung LF, Huang CY, Wu DW, Wu CH, Ho LJ. Mitochondrial protein CMPK2 regulates IFN alpha-enhanced foam cell formation, potentially contributing to premature atherosclerosis in SLE. Arthritis Res Ther. 2021;23:120.
38. Satoh M, Reeves WH. Induction of lupus-associated autoantibodies in BALB/c mice by intraperitoneal injection of pristane. J Exp Med. 1994;180:2341–6.
39. Domizio JD, Gulen MF, Saidoune F, Thacker VV, Yatim A, Sharma K, Nass T, Guenova E, Schaller M, Conrad C, et al. The cGAS-STING pathway drives type I IFN immunopathology in COVID-19. Nature. 2022;603:145–51.
40. Lai JH, Wu DW, Wu CH, Hung LF, Huang CY, Ka SM, Chen A, Chang ZF, Ho LJ. Mitochondrial CMPK2 mediates immunomodulatory and antiviral activities through IFN-dependent and IFN-independent pathways. iScience. 2021;24:102498.
41. Hsu YL, Wang MY, Ho LJ, Lai JH. Dengue virus infection induces interferon-lambda1 to facilitate cell migration. Sci Rep. 2016;6:24530.
42. Xian H, Watari K, Sanchez-Lopez E, Offenberger J, Onyuru J, Sampath H, Ying W, Hoffman HM, Shadel GS, Karin M. Oxidized DNA fragments exit mitochondria via mPTP- and VDAC-dependent channels to activate NLRP3 inflammasome and interferon signaling. Immunity. 2022;55(1370–85): e8.
43. Tumurkhuu G, Dagvadorj J, Porritt RA, Crother TR, Shimada K, Tarling EJ, Erbay E, Arditi M, Chen S. Chlamydia pneumoniae Hijacks a Host Autoregulatory IL-1beta Loop to Drive Foam Cell Formation and Accelerate Atherosclerosis. Cell Metab. 2018;28(432–48): e4.
44. Niyonzima N, Rahman J, Kunz N, West EE, Freiwald T, Desai JV, Merle NS, Gidon A, Sporsheim B, Lionakis MS, et al. Mitochondrial C5aR1 activity in macrophages controls IL-1beta production underlying sterile inflammation. Sci Immunol. 2021;6:eabf2489.
45. Lepelley A, Wai T, Crow YJ. Mitochondrial Nucleic Acid as a Driver of Pathogenic Type I Interferon Induction in Mendelian Disease. Front Immunol. 2021;12: 729763.
46. Al-Mehdi AB, Pastukh VM, Swiger BM, Reed DJ, Patel MR, Bardwell GC, Pastukh VV, Alexeyev MF, Gillespie MN. Perinuclear mitochondrial clustering creates an oxidant-rich nuclear domain required for hypoxia-induced transcription. Sci Signal. 2012;5:ra47.
47. Katsiari CG, Liossis SN, Sfikakis PP. The pathophysiologic role of monocytes and macrophages in systemic lupus erythematosus: a reappraisal. Semin Arthritis Rheum. 2010;39:491–503.
48. Kwant LE, Vegting Y, Tsang ASMWP, Kwakernaak AJ, Vogt L, Voskuyl AE, van Vollenhoven RF, de Winther MPJ, Bemelman FJ, Anders HJ, Hilhorst ML. Macrophages in Lupus Nephritis: Exploring a potential new therapeutic avenue. Autoimmun Rev. 2022;21:103211.
49. Yarilina A, Park-Min KH, Antoniv T, Hu X, Ivashkiv LB. TNF activates an IRF1-dependent autocrine loop leading to sustained expression of chemokines and STAT1-dependent type I interferon-response genes. Nat Immunol. 2008;9:378–87.
50. Aarreberg LD, Esser-Nobis K, Driscoll C, Shuvarikov A, Roby JA, Gale M Jr. Interleukin-1beta Induces mtDNA Release to Activate Innate Immune Signaling via cGAS-STING. Mol Cell. 2019;74(801–15): e6.
51. Orzalli MH, Smith A, Jurado KA, Iwasaki A, Garlick JA, Kagan JC. An Antiviral Branch of the IL-1 Signaling Pathway Restricts Immune-Evasive Virus Replication. Mol Cell. 2018;71(825–40): e6.
52. Lechner J, Malloth N, Seppi T, Beer B, Jennings P, Pfaller W. IFN-alpha induces barrier destabilization and apoptosis in renal proximal tubular epithelium. Am J Physiol Cell Physiol. 2008;294:C153–60.
53. Romero-Weaver AL, Wang HW, Steen HC, Scarzello AJ, Hall VL, Sheikh F, Donnelly RP, Gamero AM. Resistance to IFN-alpha-induced apoptosis is linked to a loss of STAT2. Mol Cancer Res. 2010;8:80–92.
54. Buang N, Tapeng L, Gray V, Sardini A, Whilding C, Lightstone L, Cairns TD, Pickering MC, Behmoaras J, Ling GS, Botto M. Type I interferons affect the metabolic fitness of CD8(+) T cells from patients with systemic lupus erythematosus. Nat Commun. 2021;12:1980.
55. Boswell J, Schur PH. Monocyte function in systemic lupus erythematosus. Clin Immunol Immunopathol. 1989;52:271–8.
56. Salmon JE, Kimberly RP, Gibofsky A, Fotino M. Defective mononuclear phagocyte function in systemic lupus erythematosus: dissociation of Fc receptor-ligand binding and internalization. J Immunol. 1984;133:2525–31.
57. Fries LF, Mullins WW, Cho KR, Plotz PH, Frank MM. Monocyte receptors for the Fc portion of IgG are increased in systemic lupus erythematosus. J Immunol. 1984;132:695–700.
58. Xu Y, Johansson M, Karlsson A. Human UMP-CMP kinase 2, a novel nucleoside monophosphate kinase localized in mitochondria. J Biol Chem. 2008;283:1563–71.
59. Chen YL, Lin DW, Chang ZF. Identification of a putative human mitochondrial thymidine monophosphate kinase associated with monocytic/macrophage terminal differentiation. Genes Cells. 2008;13:679–89.
60. Davidson A. Renal Mononuclear Phagocytes in Lupus Nephritis. ACR Open Rheumatol. 2021;3:442–50.
61. Richoz N, Tuong ZK, Loudon KW, Patino-Martinez E, Ferdinand JR, Portet A, et al. Distinct pathogenic roles for resident and monocyte-derived macrophages in lupus nephritis. JCI Insight. 2022;7(21). https://doi.org/10.1172/jci.insight.159751. https://www.ncbi.nlm.nih.gov/pubmed/36345939.
62. Arazi A, Rao DA, Berthier CC, Davidson A, Liu Y, Hoover PJ, Chicoine A, Eisenhaure TM, Jonsson AH, Li S, et al. The immune cell landscape in kidneys of patients with lupus nephritis. Nat Immunol. 2019;20:902–14.
63. Bradley SJ, Suarez-Fueyo A, Moss DR, Kyttaris VC, Tsokos GC. T Cell Transcriptomes Describe Patient Subtypes in Systemic Lupus Erythematosus. PLoS ONE. 2015;10: e0141171.
64. Cutts Z, Patterson S, Maliskova L, Taylor KE, Ye CJ, Dall'Era M, Yazdany J, Criswell LA, Fragiadakis GK, Langelier C, et al. Cell-Specific Transposable Element and Gene Expression Analysis Across Systemic Lupus Erythematosus Phenotypes. ACR Open Rheumatol. 2024;6:769–79.
65. Braunstein I, Klein R, Okawa J, Werth VP. The interferon-regulated gene signature is elevated in subacute cutaneous lupus erythematosus and discoid lupus erythematosus and correlates with the cutaneous lupus area and severity index score. Br J Dermatol. 2012;166:971–5.
66. Bulusu SN, Mariaselvam CM, Shah S, Kommoju V, Kavadichanda C, Harichandrakumar KT, Thabah M, Negi VS. Type I interferon gene expression signature as a marker to predict response to cyclophosphamide based treatment in proliferative lupus nephritis. Lupus. 2024;33:1069–81.

Publisher's Note